

**AN-NAJAH NATIONAL UNIVERSITY
FACULTY OF GRADUATE STUDIES**

**FP-LAPW calculations of the electronic properties and
structural phase transitions in CoO and CdO**

By

Kamal Falah Naji Mostafa

Supervisor

Dr. Mohammed S. Abu-Ja'far

**This Thesis is Submitted in Partial Fulfilment of the Requirements for the
Degree of Master of Science in Physics, Faculty of Graduate Studies, at An-
Najah National University, Nablus, Palestine.**

2009

Dedications



**FP-LAPW calculations of the electronic properties and structural
phase transitions in CoO and CdO**

By

Kamal Falah Naji Mostafa

This Thesis was defended successfully on 19/11/2009 and approved by

Defense Committee Members

Signature

1- Dr. Mohammed Abu Ja'far (Supervisor)

Mohid S.

2- Dr. Abdel-Rahman Abu Labdeh (External Examiner)

Abdel-Rahman

3- Dr. Musa El-Hasan (Internal Examiner)

Melhasan

Dedications

بِسْمِ اللَّهِ الرَّحْمَنِ الرَّحِيمِ

To my parents, my wife and my kids.

To every one who I love and respect.

ACKNOWLEDGEMENT

I would like to thank my teacher and supervisor Dr. Mohammed Abu-Ja'far for his support, guidance and for his help with the WIEN2K code which based on his wide experience in teaching and research. Thanks and appreciation to the defence committee members Dr. Musa El-Hasan and Dr. Abdel-Rahman Abu Labdeh for their time and patient. Also I would like to thank all the physics department members who taught me and guide me to the truth Dr. Isam Al Ashqar, Dr. Abdel-Rahman Abu Labdeh and Dr. Sami Jaber. Also I would like to thank my colleague Omar Isleem for his help and support.

Special thanks and special appreciation to the one who pushed me forward my wife Asmahan, and to my kids Hamza, Amr, Ibrahem and Ahmad for their support, encouragement and patient.

Finally, I would like to thank my parents, my brothers, and my sisters for their support.

إقرار

أنا الموقع أدناه مقدم الرسالة التي تحمل العنوان:

FP-LAPW calculations of the electronic properties and structural phase transitions in CoO and CdO

أقر بان ما اشتملت عليه هذه الرسالة إنما هي نتاج جهدي الخاص ، باستثناء ما تمت الإشارة إليه حيثما ورد ، وأن هذه الرسالة ككل ، أو أي جزء منها لم يقدم من قبل لنيل أية درجة أو لقب علمي أو بحثي لدى أي مؤسسه تعليمية أو بحثية أخرى.

Declaration

The work provided in this thesis, unless otherwise referenced, is the researcher's own work, and has not been submitted elsewhere for any other degree or qualification.

Student's name:

اسم الطالب :

Signature:

التوقيع :

Date:

التاريخ:

Table of contents

<i>Section</i>	<i>Subject</i>	<i>Page</i>
1	Introduction	1
2	Theory of calculations	7
2.1	Introduction	7
2.2	The Born-Oppenheimer approximation	8
2.3	Density Functional Theory (DFT)	10
2.4	The exchange-correlation functional	12
2.5	The Local Density Approximation (LDA)	13
2.6	Generalized Gradient Approximation (GGA)	14
2.7	Choice of method	15
2.7.1	The linearized – augmented plane wave method (LAPW)	15
2.7.2	Different implementations of augmented plane wave (APW)	18
2.7.3	The full-potential scheme	18
2.7.4	Computational aspects	19
3	Crystal Structures	21
3.1	Introduction	21
3.2	Closed-packed crystal structures	22
3.2.1	Simple cubic structure (sc)	22
3.2.2	Body-centred structure (bcc)	22
3.2.3	Face-centred cubic (fcc)	23
3.2.4	Hexagonal close packed (hcp)	23
3.3	Diatomic compounds	24

<i>Section</i>	<i>Subject</i>	<i>Page</i>
3.3.1	Sodium chloride structure (NaCl)	24
3.3.2	Cesium chloride structure (CsCl)	25
3.3.3	Zincblende structure (ZB)	26
3.3.4	Wurtzite structure (WZ)	27
4	Results and Discussions	28
4.1	Introduction	28
4.2	CdO Compound	29
4.2.1	Structural parameters for CdO compound	29
4.2.1.1	Rocksalt structure for CdO compound	29
4.2.1.2	CsCl structure for CdO compound	31
4.2.1.3	Zincblende structure for CdO compound	32
4.2.1.4	Wurtzite structure for CdO compound	34
4.2.2	Band structure for CdO compound	38
4.2.3	Phase transition pressure for CdO compound	41
4.3	CoO Compound	54
4.3.1	Structural parameters for CoO Compound	54
4.3.1.1	Rocksalt structure for CoO Compound	54
4.3.1.2	CsCl structure for CoO Compound	57
4.3.1.3	Zincblende Structure for CoO compound	57
4.3.2	The energy band gaps for CoO compound	58
4.3.3	Phase transition pressure for CoO compound	60
5	Conclusions	68
5.1	Introduction	68
5.2	Structural parameters for CdO and CoO compounds	68

<i>Section</i>	<i>Subject</i>	<i>Page</i>
5.3	The energy band gaps for CdO and CoO compounds	69
5.3.1	The energy band gaps for CdO compound	69
5.3.2	The energy band gaps for CoO compound	69
5.4	Transition pressure for CdO and CoO compounds	70
5.4.1	Transition pressure for CdO compound	70
5.4.2	Transition pressure for CoO compound	70
5.5	Ground state for CdO and CoO compounds	71
5.5.1	Ground state for CdO compound	71
5.5.2	Ground state for CoO compound	71
5.6	Nature of CdO and CoO compounds	71
5.6.1	Nature of CdO compound	71
5.6.2	Nature of CoO compound	72
	References	73

LIST OF TABLES

Number	Name	Page
Table(4.1)	Structural parameters of RS structure for CdO by GGA,LDA and W-Cohen approximations	31
Table(4.2)	Structural parameters of CsCl structure for CdO by GGA,LDA and W-Cohen approximations	32
Table(4.3)	Structural parameters of ZB structure for CdO by GGA,LDA and W-Cohen approximations	33
Table(4.4)	Finding u by GGA of WZ structure for CdO	34
Table(4.5)	Finding u by W-Cohen of WZ structure for CdO	35
Table(4.6)	Finding u by LDA of WZ structure for CdO	35
Table(4.7)	Finding c/a ratio by GGA for CdO	36
Table(4.8)	Finding c/a ratio by W-Cohen for CdO	36
Table(4.9)	Finding c/a ratio by LDA for CdO	37
Table(4.10)	Structural parameters of WZ for CdO	38
Table(4.11)	The energy band gaps for CdO in RS, CsCl, ZB and WZ structures	41
Table(4.12)	The transition pressure between the structures of CdO	53
Table(4.13)	Choosing best Rk_{\max} for CoO for RS, CsCl and ZB structures	55
Table(4.14)	Choosing best k_{points} for CsCl structure of CoO by GGA method	55
Table(4.15)	Choosing best k_{points} for RS structure of CoO by LDA method	56
Table(4.16)	Choosing best k_{points} for ZB structure of CoO by W-Cohen method	56

Table(4.17)	Structural parameters for RS structure of CoO by GGA,LDA and W-Cohen approximations	56
Table(4.18)	Structural parameters of CsCl structure for CoO by GGA,LDA and W-Cohen approximations	57
Table(4.19)	Structural parameters of ZB structure for CoO by GGA,LDA and W-Cohen approximations	57
Table(4.20)	The energy band gaps for CoO compound	58
Table(4.21)	The transition pressure between the structures of CoO compound	67

LIST OF FIGURES

Number	Name	page
Fig(2.1)	Partitioning of the unit cell into atomic spheres (I) and an interstitial region(II).	16
Fig(3.1)	Simple cubic structure (sc) packing of spheres	22
Fig(3.2)	Body-centred cubic (bcc)	23
Fig(3.3)	Face centred cubic (fcc)	23
Fig(3.4)	Hexagonal close packed (hcp)	24
Fig(3.5)	CdO compound in RS structure	25
Fig(3.6)	CdO compound in CsCl structure	26
Fig(3.7)	CdO compound in ZB structure	27
Fig(3.8)	CdO compound in WZ structure	27
Fig(4.1)	Energy versus volume for CdO in RS structure by GGA method	30
Fig(4.2)	Energy versus volume for CdO in CsCl structure by GGA method	31
Fig(4.3)	Energy versus volume for CdO in ZB structure by LDA method	33
Fig(4.4)	Band structure for CdO in ZB structure	39
Fig(4.5)	Band structure for CdO in CsCl structure	39
Fig(4.6)	Band structure for CdO in RS structure	40
Fig(4.7)	Band structure for CdO in WZ structure	40
Fig(4.8)	Equations of state for CdO in RS and CsCl by GGA method	42
Fig(4.9)	Equations of state for CdO in RS and CsCl by LDA method	43
Fig(4.10)	Equations of state for CdO in RS and CsCl by W-Cohen method	43
Fig(4.11)	Equations of state for CdO in WZ and CsCl by GGA method	44

Fig(4.12)	Equations of state for CdO in WZ and CsCl by LDA method	44
Fig(4.13)	Equations of state for CdO in WZ and CsCl for by W-Cohen method	45
Fig(4.14)	Equations of state for CdO in ZB and CsCl by GGA method	45
Fig(4.15)	Equations of state for CdO in ZB and CsCl by LDA method	46
Fig(4.16)	Equations of state for CdO in ZB and CsCl by W-Cohen method	46
Fig(4.17)	Equations of state for CdO in WZ and ZB by GGA method	47
Fig(4.18)	Equations of state for CdO in WZ and ZB by LDA method	47
Fig(4.19)	Equations of state for CdO in WZ and ZB by W-Cohen method	48
Fig(4.20)	Equations of state for CdO in ZB and RS by GGA method	49
Fig(4.21)	Equations of state for CdO in ZB and RS by LDA method	49
Fig(4.22)	Equations of state for CdO in ZB and RS by W-Cohen method	50
Fig(4.23)	Equations of state for CdO in WZ and RS by GGA method	50
Fig(4.24)	Equations of state for CdO in WZ and RS by LDA method	51
Fig(4.25)	Equations of state for CdO in WZ and RS by W-Cohen method	51
Fig(4.26)	Equations of state for CdO in RS, CsCl, ZB and WZ structures by GGA method	52
Fig(4.27)	Equations of state for CdO in RS, CsCl, ZB and WZ structures by W-Cohen method	52
Fig(4.28)	Equations of state for CdO in RS, CsCl, ZB and WZ structures by LDA method	53
Fig(4.29)	Band structure for CoO in RS structure	59
Fig(4.30)	Band structure for CoO in ZB structure	59

Fig(4.31)	Band structure for CoO in CsCl structure	60
Fig(4.32)	Equations of state for CoO in RS and CsCl by GGA method	61
Fig(4.33)	Equations of state for CoO in RS and CsCl by LDA method	61
Fig(4.34)	Equations of state for CoO in RS and CsCl by W-Cohen method	62
Fig(4.35)	Equations of state for CoO in ZB and CsCl by GGA method	62
Fig(4.36)	Equations of state for CoO in ZB and CsCl by LDA method	63
Fig(4.37)	Equations of state for CoO in ZB and CsCl by W-Cohen method	63
Fig(4.38)	Equations of state for CoO in ZB and RS by GGA method	64
Fig(4.39)	Equations of state for CoO in ZB and RS by LDA method	64
Fig(4.40)	Equations of state for CoO in ZB and RS by W-Cohen method	65
Fig(4.41)	Equations of state for CoO in RS, CsCl and ZB structures by GGA method	65
Fig(4.42)	Equations of state for CoO in RS, CsCl and ZB structures by LDA method	66
Fig(4.43)	Equations of state for CoO in RS, CsCl and ZB structures by W-Cohen method	66

FP-LAPW calculations of the electronic properties and structural phase transitions in CoO and CdO

By

Kamal Falah Naji Mostafa

Supervised by

Dr. Mohammed Abu Ja'far

Abstract

In this thesis the Full-Potential Linearized Augmented Plane-Wave (FP-LAPW) method depending on the Density Functional Theory (DFT) was used to find the atomic structures of materials, the electronic properties and to investigate the structural phase transformations of CdO and CoO compounds under high pressure, and to know the conductivity and the ground state for these compounds. In these calculations the gradient generalized approximation (GGA), the local density approximation(LDA), W-Cohen approximation have been used.

For CdO, the equations of state (EOS's) of rocksalt (RS), zincblende (ZB), cesium chloride (CsCl) and wurtzite (WZ) have been calculated. From these EOS's the transition under high pressure is occurred from rocksalt (RS) to cesium chloride (CsCl), from wurtzite (WZ) to cesium chloride (CsCl), from wurtzite (WZ) to rocksalt (RS), from zincblende (ZB) to rocksalt (RS), from zincblende (ZB) to cesium chloride (CsCl), and from wurtzite (WZ) to zincblende (ZB). The energy band gaps for all structures of CdO have been calculated. It is ~ -0.5 eV for RS structure, so this structure indicates to be a semimetal. The CsCl structure indicates to be a semimetal too, because its band gap is ~ -1.1 eV. The energy band gap is ~ 0.1 eV for ZB structure, which means the CdO compound is a semimetal in this structure. And it is ~ 0.1 eV for WZ structure, so the CdO

compound is a semimetal too. The structural properties have also been calculated for all structures. We found the rocksalt (RS) structure is the ground state for CdO compound.

The same work done for CoO and the same method with the same approximations was used, the equations of state (EOS's) of rocksalt (RS), zincblende (ZB), and cesium chloride (CsCl), have been calculated. From these EOS's, the transition under high pressure is occurred from rocksalt (RS) to cesium chloride (CsCl), from zincblende (ZB) to rocksalt (RS), and from zincblende (ZB) to cesium chloride (CsCl). The energy band gaps for all structures of CoO have been calculated. It is ($-0.5 \rightarrow -0.17$ eV) for ZB, so this structure indicates a semimetal. It is between ($0.77 \rightarrow 1.1$ eV) For CsCl, which means the CoO compound is a semimetal in this structure. Finally the energy band gaps is between ($0.15 \rightarrow 0.42$ eV) for RS structure by using LDA and W-Cohen methods, so the structure is semimetal, but it is ~ 0.01 eV by using GGA method, so this structure is a semimetal too. The structural properties have also been calculated for all structures. We found the zincblende (ZB) structure is the ground state for CoO compound.

Chapter One

Introduction

The transition metal oxides (TMO) are systems with large variability of structures and chemical bonding, which brings about an alluring of magnetic, electrical, and optical properties. A strong interaction between chemical compositions of TMO, their transport characteristics, magnetic orders and crystal structures produce a rich field for fundamental research and technological applications.

The TMO are very interesting materials, because they present many diverse physical properties that depend on the cationic species. We can find superconductivity in cuprates , ferroelectricity, piezoelectricity and high permittivity dielectricity in titanates colossal magnetoresistance (CMR) and spin polarized current in manganites, only to cite the most famous compounds. There physical properties can be turned by external parameters like: temperature, applied magnetic or electric field, doping lattice stress and strain[1].

The unique characteristics of these compounds and the increasing stringent requirement of the semiconductor industry for new of memories, smaller transistors and smart sensors make these materials very promising for future electronics. The ability of making devices with TMO like field effect transistor (FET) junctions, micro-electromechanical system is important tool for studying the physical properties of TMO and for applications.

Reversible electric charge induction by field effect devices on TMO is a particular interest for smart applications and basic science, contrary to conventional

semiconductors, oxides metals present a broad spectrum of magnetic and transport properties that are affected by their charge density, due to generally high charge density of oxides compounds, high dielectric constant barriers and strong electric field are strictly required for observing detectable modulations. Fabrication of thin film dielectric barriers presents some troubles related to the difficulty to a good stoichiometry of the barrier itself, while maintaining unaltered properties of the bottom oxide material[2].

There are several techniques to grow TMO films and to fabricate device out of them, the principle deposition techniques are sputtering, molecular beam epitaxy, pulsed laser deposition, while for micro and nano-machining ultraviolet or x ray photolithography combined with dry or wet etching, focused ion beam, electronic beam lithography, local anodic oxidation by a scanning probe microscopy are generally used.

During the last 70 years TMO have been one of the most studied class of solids, these studies have led to new ideas[3] concerning the electronic structures of TMO. Strong evidence for classification of the late 3d TMO as charge transfer gap insulators has been reported by Sawatzky and Allen [4].

II-VI, III-V and group-IV wide-gap semiconductor materials are very important because of their opto-electronic technological applications as a commercial short wavelength light-emitting diode[5], laser diode candidate by p-type doping with nitrogen, transparent conductors, solar cells, high-density optical memory, visual display [6]. This is important because of the role of the d-electrons in the Valence band in hybridization which needs to open gap at the crossing make angular momentum labelling no longer suitable[7].

A crystal is made up of a large number of interacting particles. To describe what would happen to these crystals when pressurized, many methods of different potentials and techniques[8] have been used to study the structural phase transformations of these crystals zincblende (ZB), rocksalt (RS), cesium chloride (CsCl) and wurtzite (WZ) under high pressure and deal with these problems.

For many years transparent conductive oxide layers have been studied extensively, researchers have focused on a cadmium oxides CdO because of a wide range of technical applications for instances as transparent electrodes in photovoltaic and display devices, sensors, solar cells, photo transistors, diodes, transparent electrodes, gas sensors. These applications of CdO are based on its specific optical and electrical properties. For example CdO films show high transparency in the visible region of the solar spectrum. As well as a high ohmic conductivity, the intensity of optical and electrical effects of CdO depends on the deviations from ideal CdO stoichiometry, as well as on the size and shape of the particles[9]. The CdO is n-type semiconductors that crystallizes in rocksalt structure, and presents an optical band-gap of about 2.3 eV, with an indirect band gap of 1.36eV[10]. There are some physical and chemical properties of CdO, the colour is red or brown, melting point is 1426 C, density is 8.15 g/cm³, vapour pressure is 1 mm Hg at 1000 C, insoluble in water, molar mass is 128.41g / mole [11].

There are a few researches done about CdO under high pressure. Schleife et al[12] calculated the transition pressure from RS to CsCl is happen at 85 Gpa, while Jaffe et al [13] calculated the transition pressure from RS to CsCl at 515 Gpa. The experimental value was 90.6 Gpa, and the stability of the ground state phase was RS [14]. CdO has a cubic structure of RS type at ambient conditions. Its structure remains stable up to the melting temperature at room pressure and up to 35 GPa pressure at room temperature from a previous report by Dirckamer et al [15]. In

the first-principle calculations, the potential phases such as RS, CsCl, ZB, nickel arsenide, orthorhombic cmcm and WZ structures were calculated in their equilibrium geometries and curves of the energy-volume (E-V) relationship were obtained. The bulk modulus and equilibrium lattice parameter were estimated by fitting the energy as a function of volume according to the Murnaghan equation of state (EOS) [16]. The phase transition pressure was estimated from the intersection of the E-V curves of RS and CsCl phases.

Cobalt oxide CoO also is one of the most studied transition metal oxides for numerous scientific technologies. It has many industrial applications, such as catalyst for oxygen evolution and oxygen reduction reactions [17]. It is also widely used as an electrochromic material [18], solar selective absorber, and catalyst in the hydrocracking processing of crude fuels [19], and in newly invented applications in electrochemical capacitors [20].

CoO appears as olive-green to red crystals, or greyish or black powder. It is used extensively in the ceramics industry as an additive to create blue colored glazes and enamels as well as in the chemical industry for producing cobalt(II) salt. CoO crystals adopt the rocksalt structure with a lattice constant of 4.2615 Å [21].

High pressure behaviors of wurtzite-type hexagonal CoO nanocrystals were investigated by in situ high pressure synchrotron radiation X-ray diffraction measurements up to 57.4 GPa at ambient temperature [22]. It is found that the bulk modulus of the hexagonal CoO phase is about 115 GPa at zero pressure. During compression, the hexagonal CoO phase transfers into rocksalt-type cubic phase in the pressure range of 0.8-6.9 GPa. The volume collapse accompanied by the transition was estimated to be about 20%. This is an irreversible phase transformation, that is, the cubic CoO phase remains after pressure release. Based on the data of peak width vs

pressure, a cubic-to-rhombohedral phase transition was detected for the nanocrystalline cubic CoO phase with the transition pressure of about 36 Gpa, lower than 43 Gpa for bulk cubic CoO phase. The bulk modulus of the nanocrystalline cubic CoO phase of about 258 Gpa is larger than 180 Gpa for the corresponding bulk cubic CoO phase[23].

Density-functional theory (DFT) provides a foundation for modern electronic structure calculations, and the local-density approximation (LDA) and the generalized gradient approximation (GGA) are an efficient methods to calculate the ground state of material. Time-dependent DFT can in principle describe the excited state [24]. In this study we are going to use the full-potential linearized augmented plane wave (FP-LAPW), implemented in WIEN2K computer code [25], within the LDA, GGA and the improved W-GGA approximations. Using FP-LAPW method, the Kohn-Sham equation can be solved, in which the wave function is expanded in atomic orbitals in spherical regions around the atomic positions, while in the region between the spheres. it is expanded in plane waves. The wave functions and their derivatives are made continuous at the boundary of the spheres.

The FP-LAPW method places no restrictions on the form of crystalline potential and is known to yield reliable structural parameters for semiconductors, metals, and insulators. WIEN2K allows us to perform electronic structure calculations of solids using DFT , and it is based on FP-LAPW one among the most accurate schemes for band structure calculation.

The objects of this study are to:

- 1- calculate the structural parameters of the zincblende (ZB), rocksalt(RS), cesium chloride(CsCl) and wurtzite(WZ) phases of CdO compound.
- 2- calculate the structural parameters of the ZB, RS, CsCl and WZ phases for CoO compound.
- 3- determine the equations of state of ZB, RS, CsCl and WZ phases of CdO and CoO by calculating the total energy at different volumes and fitting the calculated values to Murnaghan's EO'S .
- 4-determine the transition pressure of WZ to RS, ZB to RS and WZ to ZB structural phases transformations for CdO and CoO.
- 5-determine the band structure of ZB, RS, CsCl and WZ phases of CdO and CoO.

This thesis is organized as follows:

In chapter 2 we describe the Density Functional Theory and the method which we used in the calculations. In chapter 3 we describe the crystal structures and its phases . In chapter 4 we discuss and report our results. In chapter 5 we give the summery of our main results and conclusions.

Chapter Two

Theory of calculations

2.1 Introduction

Solid materials and their mechanical properties are of great technological interest. They are governed by very different length and time scales which may differ by many orders of magnitude depending on their applications. Let us focus on the length scale, where from meters (m) down to micrometers (μ). Classical mechanics and continuum models are the dominating concepts to investigate the properties of the corresponding materials. However, when one comes to the nanometer (nm) scale or atomic dimensions measured in \AA , the mechanical properties are determined by the electronic structure of the solid. In the development of modern materials an understanding on an atomic scale is frequently essential in order to replace trial and error procedures by a systematic materials design. In this context the electronic properties of solids need to be described by a quantum mechanical treatment. Modern devices in the electronic industry provide such an example, where the increased miniaturization is one of the key advances. Other applications are found in the area of magnetic recording or other storage media. One possibility to study complex systems that contain many atoms is to perform computer simulations. Calculation of solids in general (metals, insulators, minerals, etc.) can be performed with a variety of methods from classical to quantum mechanical (QM) approaches. The former are force field or semi-empirical schemes, in which the forces that determine the interactions between the atoms are parameterized in such a way to reproduce a series of experimental data such as equilibrium geometries, bulk moduli or special vibrational frequencies (phonons). These schemes have reached a high level of sophistication and are often useful within a given class of materials

provided good parameters are already known from closely related systems. If, however, such parameters are not available, or if a system shows unusual phenomena that are not yet understood, one often must rely on ab initio calculations. They are more demanding in terms of computer requirements and thus allow only the treatment of smaller unit cells than semi-empirical calculations. The advantage of first-principle (ab initio) methods lies in the fact that they do not require any experimental knowledge to carry out such calculations. The fact that electrons are indistinguishable and are Fermions requires that their wave functions must be anti-symmetric when two electrons are interchanged. This situation leads to the phenomenon of exchange and correlation. There are two types of approaches for a full quantum mechanical treatment, Hartree Fock (HF) and the Density Functional Theory (DFT). The traditional scheme is the HF method which is based on wave function description [26].

2.2 The Born-Oppenheimer approximation

A solid is a collection of heavy, positively charged particles (nuclei) compared to lighter, negatively charged particles (electrons). If the structure composed of N nuclei and each has Z electrons, then, the theorists came face to face with a problem of N (nuclei) + ZN (electrons) electromagnetically interacting particles. This is a many-body problem, and because these particles are so light compared with classical scale, it is a quantum many body problem. In principle, to study the materials and their properties, the theorist has to solve the time independent Schrödinger equation.

$$\hat{H}\Psi = E\Psi \quad (2.1)$$

Here, Ψ is the wave function of all participating particles and \hat{H} is the exact many-particle Hamiltonian for this system.

$$\hat{H} = \frac{\hbar^2}{2} \sum_i \frac{\nabla_{R_i}^2}{M_i} - \frac{\hbar^2}{2} \sum_i \frac{\nabla_{r_i}^2}{m_i} - \frac{1}{4\pi\epsilon_0} \sum_{i,j} \frac{e^2 Z_i}{|\vec{R}_i - \vec{r}_j|} + \frac{1}{8\pi\epsilon_0} \sum_{i \neq j} \frac{e^2}{|\vec{r}_i - \vec{r}_j|} + \frac{1}{8\pi\epsilon_0} \sum_{i \neq j} \frac{e^2 Z_i Z_j}{|\vec{R}_i - \vec{R}_j|} \quad (2.2)$$

The mass of the nucleus at R_i is M_i , the electrons have mass m_e and are at r_i . The first term is the kinetic energy operator for the nuclei (T_n), the second for the electrons (T_e). The last three terms describe the Coulomb interaction between electrons and nuclei (V_{en}), between electrons and other electrons (V_{ee}), and between nuclei and other nuclei (V_{nn}). It is out of question to solve this problem exactly[27].

The nuclei are much heavier and therefore much slower than the electrons. We can hence ‘freeze’ them at fixed positions and assume the electrons to be in instantaneous equilibrium with them. In other words: only the electrons are kept as players in our many body problem [28]. The nuclei are deprived from this status, and reduced to a given source of positive charge, they become ‘external’ to the electron cloud. After having applied this approximation, we are left with a collection of NZ interacting negative particles, moving in the (now external or given) potential of the nuclei. The nuclei do not move any more, their kinetic energy is zero and the first term disappears. The last term reduces to a constant. We are left with the kinetic energy of the electron gas, the potential energy due to electron-electron interactions and the potential energy of the electrons in the (now external) potential of the nuclei. We write this formally as:

$$H = \hat{T} + \hat{V} + \hat{V}_{ext} \quad (2.3)$$

It is interesting to note here that the kinetic and electron-electron terms of 2.3 depend only on the fact that we are dealing with a many-electron system (and not with a many-proton system for instance, where the strong nuclear force would play

a role). They are independent of the particular kind of many-electron system [29]. This part is universal System-specific information (which nuclei, and on which positions) is given entirely by V_{ext} .

2.3 Density Functional Theory (DFT)

The well-established scheme to calculate electronic properties of solids is based on DFT, for which Walter Kohn has received the Nobel Prize in chemistry in 1998. DFT is a universal approach to the quantum mechanical many-body problem, where the system of interacting electrons is mapped in a unique manner onto an effective non-interacting system with the same total density. Hohenberg and Kohn [30] have shown that the ground state electron density ρ (in atoms, molecules or solids) uniquely defines the total energy E_{tot} of a system and is a functional $E_{tot}(\rho)$ of the density:

$$E_{tot}(\rho) = T_s(\rho) + E_{ee}(\rho) + E_{Ne}(\rho) + E_{xc}(\rho) + E_{NN} \quad (2.4)$$

The different electronic contributions are conventionally labeled as, respectively, the kinetic energy (of the non-interacting particles), the electron–electron repulsion, nuclear–electron attraction, and exchange–correlation energies. The last term corresponds to the repulsive Coulomb energy of the fixed nuclei E_{NN} . According to the variational principle a set of effective one-particle Schrödinger equations, the so-called Kohn–Sham (KS) equations [31], must be solved. Its form is

$$\left[-\frac{1}{2} \nabla^2 + V_{eff}(\vec{r}) + V_o(\rho(\vec{r})) + V_{no}(\rho(\vec{r})) \right] \phi_i(\vec{r}) = \epsilon_i \phi_i(\vec{r}) \quad (2.5)$$

when written in Rydberg atomic units for an atom with the obvious generalization to molecules and solids. The four terms represent the kinetic energy operator, the external potential from the nucleus, the Coulomb-, and

exchange-correlation potential, V_C and V_{xc} : The KS equations must be solved iteratively till self-consistency is reached. The iteration cycles are needed because of the interdependence between orbitals and potential. In the KS scheme the electron density is obtained by summing over all occupied states, i.e., by filling the KS orbitals (with increasing energy) according to the aufbau principle.

$$\rho(\vec{r}) = \sum_i |\phi_i(\vec{r})|^2 \quad (2.6)$$

From the electron density the V_C and V_{xc} potentials for the next iteration can be calculated, which define the KS orbitals. This closes the self consistency cycle (SCF) loop. The exact functional form of the potential V_{xc} is not known and thus one needs to make approximations. Early applications were done by using results from quantum Monte Carlo calculations for the homogeneous electron gas, for which the problem of exchange and correlation can be solved exactly, leading to the original local density approximation (LDA). LDA works reasonably well but has some shortcomings mostly due to the tendency of over binding, which cause e.g., too small lattice constants.

Modern versions of DFT, especially those using the generalized gradient approximation (GGA), improved the LDA by adding gradient terms of the electron density and reached (almost) chemical accuracy, as for example the version by Perdew, et al [32].

In the study of large systems the strategy differs for schemes based on HF or DFT. In HF based methods the Hamiltonian is well defined but can be solved only approximately (e.g., due to limited basis sets). In DFT, however, one must first choose the functional that is used to represent the exchange and correlation effects (or approximations to them) but then one can solve this effective Hamiltonian almost exactly, i.e., with very high precision. Thus in both cases an

approximation enters (either in the first or second step) but the sequence is reversed. This perspective illustrates the importance in DFT calculations of improving the functional, since this defines the quality of the calculation.

2.4 The exchange-correlation functional

Apart from the preceding Born-Oppenheimer approximation, no other approximations were made, but we neglected so far the fact that we do not know the exchange-correlation functional [33]. A widely used approximation-called the Local Density Approximation (LDA) is to postulate that the exchange-correlation functional has the following form:

$$E_{xc}^{LDA} = \int \rho(\vec{r}) \epsilon_{xc}(\rho(\vec{r})) d\vec{r} \quad (2.7)$$

The function (not: functional) $\epsilon_{xc}(\rho)$ for the homogeneous electron gas, (The homogeneous electron gas, uniform electron gas) is an imaginary solid where all nuclear charge is homogeneously smeared out over space. This material is completely isotropic, and identical on every length scale. Therefore the electron density is constant: $\rho = N/V$, with N the number of electrons in the material, and V its volume. The parameter ρ is the only thing we need to specify a particular homogeneous electron gas completely. If the electrons do not interact, we are in the case of the free electron gas, which can be solved analytically in a straightforward way. The problem is much more difficult for an interacting electron gas. Here numerical calculations for the total energy are possible by quantum Monte-Carlo. Subtracting the non-interacting kinetic energy and the Hartree energy gives a numerical result for the exchange-correlation energy. If this is done for several densities ρ the function $\epsilon_{xc}(\rho)$ is obtained. Note that $\epsilon_{xc}(\rho)$ is a function of ρ , not a functional) and is numerically known.

This postulate is somehow reasonable: it means that the exchange-correlation energy due to a particular density $\rho(\vec{r})$ could be found by dividing the material in

infinitesimally small volumes with a constant density [34]. Each such volume contributes to the total exchange correlation energy by an amount equal to the exchange correlation energy of an identical volume filled with a homogeneous electron gas, which has the same overall density as the original material has in this volume. No law of nature guarantees that the true E_{xc} is of this form, it is only a reasonable guess. By construction, LDA is expected to perform well for systems with a slowly varying density. But rather surprisingly, it appears to be very accurate in many other (realistic) cases too. A next logical step to improve on LDA, is to make the exchange-correlation contribution of every infinitesimal volume not only dependent on the local density in that volume, but also on the density in the neighboring volumes. In other words, the gradient of the density will play a role. This approximation is therefore called the Generalized Gradient Approximation (GGA). Although GGA performs in general slightly better than LDA, there are a few draw backs. There is only one LDA exchange-correlation functional, because there is a unique definition for ϵ_{xc} . But there is some freedom to incorporate the density gradient, and therefore several versions of GGA exist. Moreover, in practice one often fits a candidate GGA-functional with (hopefully only a few) free parameters to a large set of experimental data on atoms and molecules. The best values for these parameters are fixed then, and the functional is ready to be used routinely in solids. Therefore such a GGA-calculation is strictly spoken not an ab-initio calculation, as some experimental information is used. Nevertheless, there exist GGA's that are parameter free [35].

2.5 The Local - Density Approximation (LDA)

The local-density approximation (LDA) is an approximation of the exchange-correlation (XC) energy functional in density functional theory (DFT) by taking the XC energy of an electron in a homogeneous electron gas of a density equal

to the density at the electron in the system being calculated (which in general is inhomogeneous). This approximation was applied to DFT by Kohn and Sham in an early paper[36]. The Hohenberg-Kohn theorem states that the energy of the ground state of a system of electrons is a functional of the electronic density, in particular the exchange and correlation energy is also a functional of the density (this energy can be seen as the quantum part of the electron-electron interaction). This XC functional is not known exactly and must be approximated [37]. LDA is the simplest approximation for this functional, it is local in the sense that the electron exchange and correlation energy at any point in space is a function of the electron density at that point only[38]. The LDA functional assumes that the per-electron exchange-correlation energy at every point in space is equal to the per-electron exchange-correlation energy of a homogeneous electron gas[39]. The XC correlation functional is the sum of a correlation functional and an exchange functional [40]

$$E_{xc}=E_x +E_c \tag{2.8}$$

2.6 Generalized Gradient Approximation (GGA)

Many modern codes using DFT now use more advanced approximations to improve accuracy for certain physical properties. The DFT calculations in this study have been made using the Generalized Gradient Approximation (GGA) . As stated above, the LDA uses the exchange-correlation energy for the uniform electron gas at every point in the system regardless of the homogeneity of the real charge density. For non uniform charge densities the exchange-correlation energy can deviate significantly from the uniform result. This deviation can be expressed in terms of the gradient and higher spatial derivatives of the total charge density. The GGA uses the gradient of the charge density to correct for this deviation. For systems where the charge density is slowly varying, the GGA

has proved to be an improvement over LDA[41]. Generalized gradient approximations (GGA's) seek to improve upon the accuracy of the local-spin-density (LSD) approximation in electronic-structure calculations.

2.7 Choice of method

As a consequence of the aspects described above different methods have their advantages or disadvantages when it comes to compute various quantities. For example, properties that rely on the knowledge of the density close to the nucleus (hyperfine fields, electric field gradients, etc.), require an all-electron description rather than a pseudo-potential approach with un-physical wave functions near the nucleus. On the other hand for studies, in which the shape (and symmetry) of the unit cell changes, the knowledge of the corresponding stress tensor is needed for an efficient structural optimization. These tensors are much easier to obtain in pseudo-potential schemes and thus are available there. In augmentation schemes such algorithms become more tedious and consequently are often not implemented. On the other hand all-electron methods do not depend on choices of pseudo-potentials and contain the full wave function information. Thus the choice of method for a particular application depends on the property of interest and may affect the accuracy, ease or difficulty to calculate a given property.

2.7.1 The linearized-augmented plane wave method (LAPW)

One among the most accurate schemes for solving the Kohn–Sham equations is the full-potential linearized-augmented-plane wave (FP-LAPW) method suggested by Andersen [42] on which our WIEN code is based. In the LAPW method [43] a basis set is introduced that is especially adapted to the problem by

dividing the unit cell into (I) non-overlapping atomic spheres (centered at the atomic sites) and (II) an interstitial region Figure 2.1. For the construction of basis functions but only for that purpose the Muffin-tin Approximation (MTA) is used according to which the potential is assumed to be spherically symmetric within the atomic spheres but constant outside. In the two types of regions different basis sets are used.

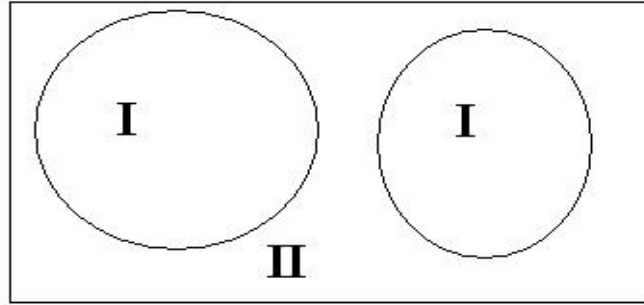


Figure 2.1 Partitioning of the unit cell into atomic spheres (I) and an interstitial region (II).

(I) inside atomic sphere t , of radius R_t , a linear combination of radial functions times spherical harmonics $Y_{lm}(r)$ is used

$$\phi_{k_n} = \sum_{lm} [A_{lm,k_n} u_l(r, E_l) + B_{lm,k_n} \dot{u}_l(r, E_l)] Y_{lm}(\theta) \quad (2.9)$$

where $u_l(r, E_l)$ is the (at the origin) regular solution of the radial Schrödinger equation for energy E_l (usually chosen at the center of bands with the corresponding l -like character) and $\dot{u}_l(r, E_l)$ is the energy derivative of u_l evaluated at the same energy E_l . A linear combination of these two functions linearized the energy dependence of the radial function; the coefficients A_{lm} and B_{lm} are functions of k_n (see below) and are determined by requiring that this basis function matches (in value and slope) the Plane Wave (PW) labelled with

k_n , the corresponding basis function of the interstitial region. The functions u_i and \tilde{u}_i are obtained by numerical integration of the radial Schrödinger equation on a radial mesh inside the sphere.

(II) in the interstitial region a PW expansion is used

$$\phi_{k_n} = \frac{1}{\sqrt{V}} e^{ik_n \cdot r} \quad (2.10)$$

where $k_n = k + K_n$; K_n are the reciprocal lattice vectors and k is the wave vector inside the first Brillouin zone. Each PW is augmented by an atomic like function in every atomic sphere as described above. The solutions to the Kohn–Sham equations are expanded in this combined basis set of LAPW's according to the linear variation method

$$\psi_k = \sum_n c_n \phi_{k_n} \quad (2.11)$$

and the coefficients C_n are determined by the Rayleigh–Ritz variational principle. The convergence of this basis set is controlled by a cutoff parameter $R_{mt}K_{max} = 6-9$, where R_{mt} is the smallest atomic sphere radius in the unit cell and K_{max} is the magnitude of the largest K_n vector in equation (2.13). In order to improve upon the linearization (i.e. to increase the flexibility of the basis) and to make possible a consistent treatment of semi-core and valence states in one energy window (to ensure orthogonality) additional (k_n independent) basis functions can be added. They are called local orbitals (LO) [44] and consist of a linear combination of two radial functions at two different energies (e.g. at the 3s and 4s energies) and one energy derivative (at one of these energies):

$$\phi_{lm}^{LO} = \sum_{lm} \left[A_{lm,k_n} u_l(r, E_{1,l}) + B_{lm,k_n} \tilde{u}_l(r, E_{1,l}) + C_{lm} u_l(r, E_{2,l}) \right] Y_{lm}(\hat{r}) \quad (2.12)$$

The coefficients A_{lm} , B_{lm} and C_{lm} are determined by the three requirements that ϕ_{lm}^{LO} should be normalized and has zero value and slope at the sphere boundary.

2.7.2 Different implementations of augmented plane wave (APW)

The energy dependence of the atomic radial functions described above can be treated in different ways. In APW this is done by finding the energy that corresponds to the eigen-energy of each state. This leads to a non-linear eigenvalue problem, since the basis functions become energy dependent. In LAPW a linearization of the energy dependence is introduced by solving the radial Schrödinger equation for a fixed linearization energy but adding the energy derivative of this function. The corresponding two coefficients can be chosen such as to match (at the atomic sphere boundary) the atomic solution to each PW in value and slope, which determine the two coefficients of the function and its derivative. LAPW leads to a standard general eigenvalue problem but the PW basis is less efficient than in APW. A new scheme, APW plus local orbitals, combines the advantages of both methods. The matching is only done in value, but this new scheme leads to a significant speed-up of the method (up to an order of magnitude) while keeping the high accuracy of LAPW. A description of these three types of schemes (APW, LAPW, APW+ lo) mentioned above is the basis for the new WIEN2k code [45].

2.7.3 The full-potential scheme

The muffin-tin approximation (MTA) was frequently used in the 1970s and works reasonable well in highly coordinated (metallic) systems such as face centered cubic (fcc) metals. However, for covalently bonded solids, open or layered structures, MTA is a poor approximation and leads to serious discrepancies with experiment. In all these cases a treatment without any shape approximation is essential. Both, the potential and charge density, are expanded

into lattice harmonics (inside each atomic sphere) and as a Fourier series (in the interstitial region).

$$V(r) = \begin{cases} \sum_{LM} V_{LM}(r) Y_{LM}(\theta) & \text{inside sphere} \\ \sum_K V_K e^{iK \cdot r} & \text{outside sphere} \end{cases} \quad (2.13)$$

Thus their form is completely general so that such a scheme is termed full-potential calculation. The choice of sphere radii is not very critical in full potential calculations in contrast to MTA, in which one would obtain different radii as optimum choice depending on whether one looks at the potential (maximum between two adjacent atoms) or the charge density (minimum between two adjacent atoms). Therefore in MTA one must make a compromise but in full-potential calculations one can efficiently handle this problem.

2.7.4 Computational aspects

In the newest version WIEN2k [25] the alternative basis set (APW + lo) is used inside the atomic spheres for those important orbitals (partial waves) that are difficult to converge (outermost valence p-, d-, or f-states) or for atoms, where small atomic spheres must be used. For all the other partial waves the LAPW scheme is used. In addition new algorithms for solving the computer intensive general eigenvalue problem were implemented. The combination of algorithmic developments and increased computer power has led to a significant improvement in the possibilities to simulate relatively large systems on moderate computer hardware. Now personal computers (PCs) or a cluster of PCs can be efficiently used instead of the powerful workstations or supercomputers that were needed about a decade ago. Several considerations are essential for a modern computer code and were made in the development of the new WIEN2k package [25].

Accuracy is extremely important in the present case. It is achieved by the well-balanced basis set, which contains numerical radial functions that are recalculated in each iteration cycle. Thus these functions adapt to effects due to charge transfer or hybridization, are accurate near the nucleus and satisfy the cusp condition.

The PW convergence can essentially be controlled by one parameter, namely the cutoff energy corresponding to the highest PW component. There is no dependence on selecting atomic orbitals or pseudo-potentials. It is a full potential and all electron method. Relativistic effects (including spin orbit coupling) can be treated with a quality comparable to solving Dirac's equation.

Efficiency and good performance should be as high a possible. The smaller matrix size of the new mixed basis APW+ lo/LAPW helps to save computer time or allows studying larger systems.

Chapter Three

Crystal Structures

3.1 Introduction

Lattices are regular arrays of imaginary points in space. A real crystal has atoms associated with these points. The location of an atom of element at each lattice point, the atoms of the element is said to be the basis associated with each lattice point:

$$\text{Lattice} + \text{Basis} = \text{Crystal Structure}$$

The basis need not consist of just one atom, consider a motif consisting of a pair of an element atoms, with coordinates $(0, 0, 0)a$ and $(0.25, 0.25, 0.25)a$ relative to a lattice point. A crystal structure is composed of a basis, a set of atoms arranged in a particular way, and a lattice. Basis is located upon the points of a lattice, which is an array of points repeating periodically in three dimensions. The points can be thought of as forming identical tiny boxes, called unit cells, that fill the space of the lattice. The lengths of the edges of a unit cell and the angles between them are called the lattice parameters. The symmetry properties of the crystal are embodied in its space group [47]. A crystal's structure and symmetry play a role in determining many of its properties, such as electronic band structure, and optical properties.

3.2 Closed-packed crystal structures

3.2.1 Simple cubic structure (sc)

It might be thought that the simplest cubic packing would simply have a cubic unit cell with only one lattice point in the unit cell. This structure is shown in Figure 3.1, each atom has six nearest neighbours, touching along the cube edges. In spite of its apparent simplicity, there is only one element that crystallises with the simple cubic structure, namely polonium.

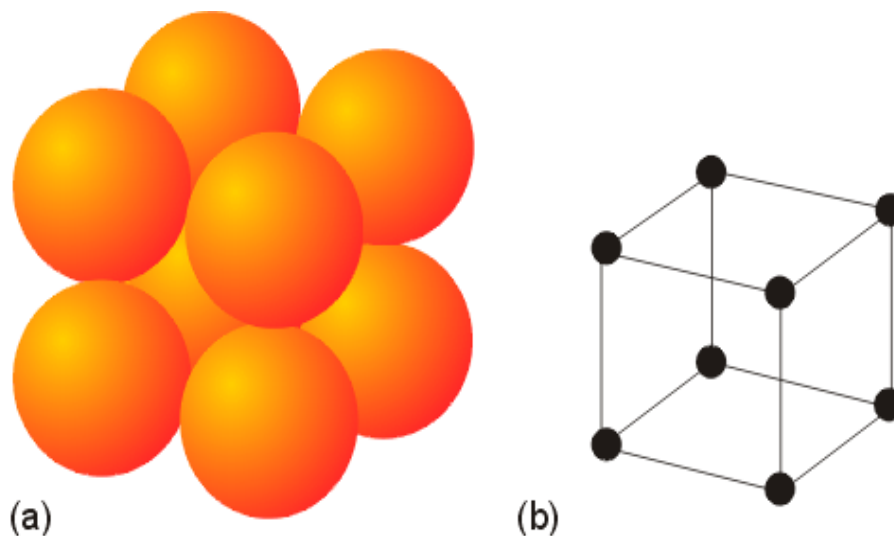


Figure 3.1 Simple cubic (sc) packing of spheres

3.2.2 Body-centred cubic (bcc)

Several metallic elements, including some of the alkali metals and iron, have a packing that is a little less efficient than close packing. This packing is easily described as a cubic cell with a second atom in the middle, with each atom having eight touching neighbouring atoms. This structure is called body-centred cubic abbreviated as bcc, and is shown in Figure 3.2.

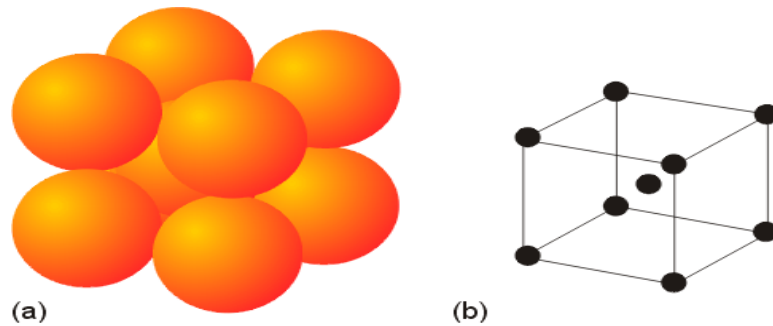


Figure 3.2 Body- centred cubic (bcc).

3.2.3 Face-centred cubic (fcc)

The face-centred cubic is one of the most common types of crystal lattices. In addition to the eight atoms located at the corners of the cube, the face centred cell contains an additional atom in each face of the cube, the face-centred cube lattice is adopted by many element. this structure is shown in Figure 3.3.

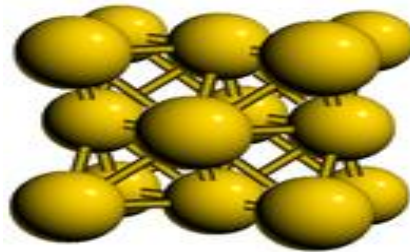


Figure 3.3 face-centred cubic (fcc)

3.2.4 Hexagonal close packed (hcp)

In hexagonal closed packed (hcp) arrangement of atoms, the unit cell consists of three layer of atoms, the tope and the bottom layers contains six atoms at the corners of hexagon and one atom at the centre of each hexagon, the middle layer contains three atoms nestled between atoms of the top and bottom layers, hence the name closed packed.

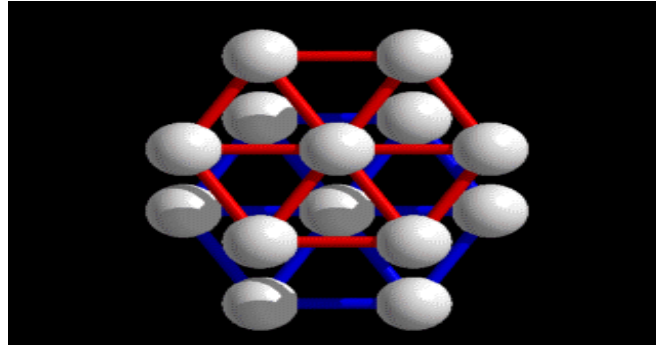


Figure 3.4 Hexagonal close packed (hcp)

3.3 Diatomic compounds

The crystal structure has two main components, the lattice that gives the periodicity and the contents the unit cell associated with each lattice point. For the bcc structure the primitive unit cell contained just one atom. However for hcp structure the unit cell contains two atoms, and for other structures of the elements there are even more atoms in the unit cell. All the structures we now consider have more than one type of atom in the unit cell. All the principles we have discussed with regard to the crystal structure of the elements. The most common structures of the diatomic compounds are all cubic and named sodium chloride structure (NaCl), cesium chloride structure (CsCl) and zinc sulfide (ZnS) structures.

3.3.1 Sodium chloride structure (NaCl)

The NaCl structure has a fcc lattice. There is one type of atom at position $(0, 0, 0)a$ and another position $(0.5, 0.5, 0.5)a$, the other atom in the conventional cubic unit cell are generated by addition of the three vectors to the face centres, namely by addition of $(0.5, 0.5, 0)a$, $(0.5, 0, 0.5)a$, and $(0, 0.5, 0.5)a$ to the two initial atomic positions. The NaCl structure is shown in the Figure 3.8, an easy way to describe this structure is to begin with one atom type in a cubic closest-packed structure (ccp). There is a set of equivalent empty sites with coordinates

$(0.5, 0, 0)a$, $(0, 0.5, 0)a$, $(0, 0, 0.5)a$ and $(0.5, 0.5, 0.5)a$. The sites are at the centres of groups of six ions with perfect octahedral arrangement. In the NaCl structure, the sites are occupied by the second set of atoms. As a results of the symmetry both types of atoms have six neighbours of the other type with perfect octahedral arrangement. The space group of RS state is $Fm\bar{3}m$ with number 225 and the primitive vectors for RS are :

$$\vec{a}_1 = \frac{a}{2} \hat{y} + \frac{a}{2} \hat{z} \quad \vec{a}_2 = \frac{a}{2} \hat{x} + \frac{a}{2} \hat{z} \quad \vec{a}_3 = \frac{a}{2} \hat{x} + \frac{a}{2} \hat{y} \quad (3.1)$$

where a is the lattice constant.

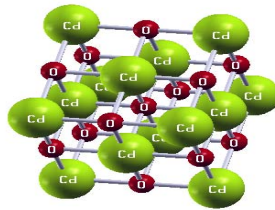


Figure 3.5 CdO compound in RS structure.

3.3.2 Cesium Chloride structure (CsCl)

The CsCl structure appears to related to the bcc packing, the unit cell of a cube, with an atom of one type at the origin, and another type of atom in the centre of the cube. Because the two atoms are different, the site at the centre of the unit cell is no longer another lattice point, and the CsCl structure must not be confused with the bcc lattice. The lattice type is therefore primitive cubic. The CsCl structure is shown in Figure 3.6 , each atom has eight neighbour of opposite type. the space group of ZB state is $F43\bar{m}$ with number 221 and the primitive vectors of ZB are:

$$\vec{a}_1 = \frac{a}{2} \hat{y} + \frac{a}{2} \hat{z} \quad \vec{a}_2 = \frac{a}{2} \hat{x} + \frac{a}{2} \hat{z} \quad \vec{a}_3 = \frac{a}{2} \hat{x} + \frac{a}{2} \hat{y} \quad (3.2)$$

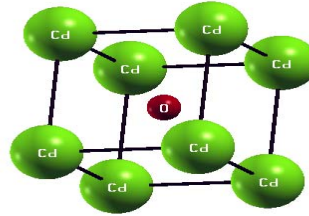


Figure 3.6 CdO compound in CsCl structure.

3.3.3 Zincblende structure (ZB)

The cubic ZnS structure is related to the diamond structure. The lattice is fcc, in the diamond structure we started from the ccp structure, and added a second set of atoms of one of the two sets of tetrahedral sites. In ZnS structure one type of atom occupies the initial ccp arrangement, with coordinates $(0, 0, 0)a$ etc...., and another type of atom occupies one of the set of tetrahedral sites at $(0.25, 0.25, 0.25)a$ etc. The ZB structure is shown in Figure 3.7, the space group of ZB state is $F43_m$ with number 216 and the primitive vectors of ZB are:

$$\vec{a}_1 = \frac{a}{2} \hat{y} + \frac{a}{2} \hat{z} \quad \vec{a}_2 = \frac{a}{2} \hat{x} + \frac{a}{2} \hat{z} \quad \vec{a}_3 = \frac{a}{2} \hat{x} + \frac{a}{2} \hat{y} \quad (3.3)$$

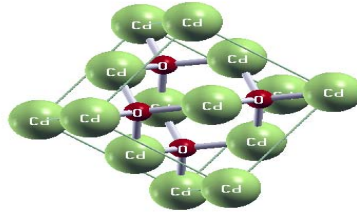


Figure 3.7 CdO compound in ZB structure.

3.3.4 Wurtzite structure (WZ)

Zinc sulfide crystallizes in two different forms: Wurtzite and Zincblende. If the sulfide ions originally adopt a hexagonal closest-packed structure, the ZnS crystal is Wurtzite. But if the sulfide ions originally adopt a cubic closest-packed structure, the ZnS crystal is Zinc Blende. In the wurtzite structure the basis: Zn at $(1/3, 2/3, 0)a$ and S at: $(1/3, 2/3, u)a$. The space group of WZ structure is $P63-mc$ with number 186 and the primitive vectors are

$$\vec{a}_1 = \frac{a}{2}\hat{x} + \frac{\sqrt{3}}{2}a\hat{y} \quad \vec{a}_2 = \frac{a}{2}\hat{x} - \frac{\sqrt{3}}{2}a\hat{y} \quad \vec{a}_3 = c\hat{z} \quad (3.4)$$

The metal oxides such as CdO adopt the wurtzite structure as shown in Figure 3.8.

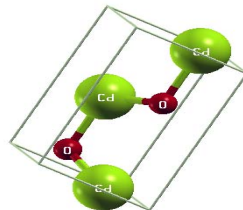


Figure 3.8 CdO compound in WZ structure.

Chapter Four

Results and Discussions

4.1 Introduction

The transition metal oxides are very important to be studied under high pressure because of the role that the d-electrons play in hybridization, covalent bonds, polarity and narrow energy band gap, where few valence electrons will gain enough energy to make transition, and for many applications for these compounds.

Materials at high pressure occur at the centres of planets and stars, but high pressure may also be applied to small laboratory samples in controlled manner using devices such as the diamond anvil (DAC). The static pressure applied in a DAC is a continuously variable parameter which can be used for systematic studies of the parameters of solids as a function of the inter-atomic distances. One of the interesting phenomena that may occur under applied pressure is a sudden change in the arrangement of the atom, i.e., structural phase transition. The Gibbs free energies of the different possible arrangement of atoms vary under compression, and at some stage it becomes favourable for material to change the type of atomic arrangement. A phase transition is said to have occurred if the change is discontinuous or continuous but with a change in crystal symmetry. The pressures achieved in a DAC can lead to a reduction in the volume by more than a factor of 2, causing enormous changes to the inter-atomic bonding[48].

4.2 CdO compound

The main aim of studying this compound is to investigate the stability of its ground state, and studying its structural phases, Rocksalt (RS), Cesium Chloride (CsCl), Zincblende (ZB) and Wurtzite (WZ). The structural parameters and the energy band gaps for each phase are calculated using the FP-LAPW approach depending on the density functional theory using GGA, LDA and W-Cohen. We also studied the transition pressure between its structures, from RS to CsCl, WZ to CsCl, WZ to RS, WZ to ZB, ZB to CsCl, and from ZB to RS structures.

4.2.1 Structural parameters for CdO compound

One of the main aim of our study is to calculate the structural parameters of CdO in the RS, CsCl, ZB, and wurtzite structures by using FP-LAPW in GGA, LDA, and W-Cohen methods. We can obtain the lattice constants a , b and c , bulk modulus B , and first derivative of the bulk modulus B' for CdO structures which is called the structural parameters.

4.2.1.1 Rocksalt structure for CdO compound

We found the lattice parameters for CdO in RS structure by GGA, LDA, and W-Cohen. The position of Cd is $(0,0,0)$ a and the position of O is $(0.5, 0.5, 0.5)$ a , $R_{mt} = 2.05$ a.u for Cd and $R_{mt} = 1.75$ a.u for O. The suitable R_{kmax} of RS structure was found to be 8 for LDA and W-Cohen methods, while it was 8.5 for GGA method. The suitable k -point is 4500 with reduced $k_{point} = 120$ in the irreducible Brillouin zone. The Brillouin zone integrations were performed with a $16 \times 16 \times 16$ K-mesh. G_{max} was 16 for GGA, but it was 15 for W-Cohen and 14 for LDA.

The structural parameters are found from optimizing job by fitting the results with Murnaghan's equation of state and plotting the energy versus volume graph.

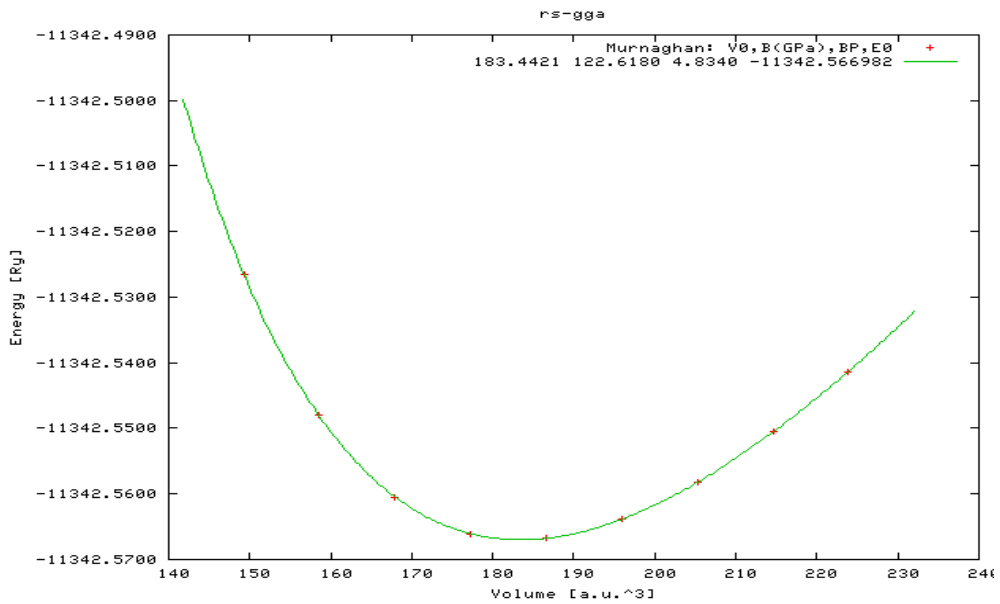


Figure 4.1 Energy versus volume for CdO in RS structure by GGA method.

From figure 4.1 we found the minimum volume V , bulk modulus B , first derivative of the bulk modulus B' and minimum energy E .

The volume of the unit cell for RS structure is

$$V = \frac{a^3}{4} \quad (4.1)$$

Then we can write a as

$$a = [4V]^{1/3} \quad (4.2)$$

where V is the volume of the unit cell, and $a = b = c$ are the lattice parameters.

Table 4.1 shows the structural parameters in RS structure.

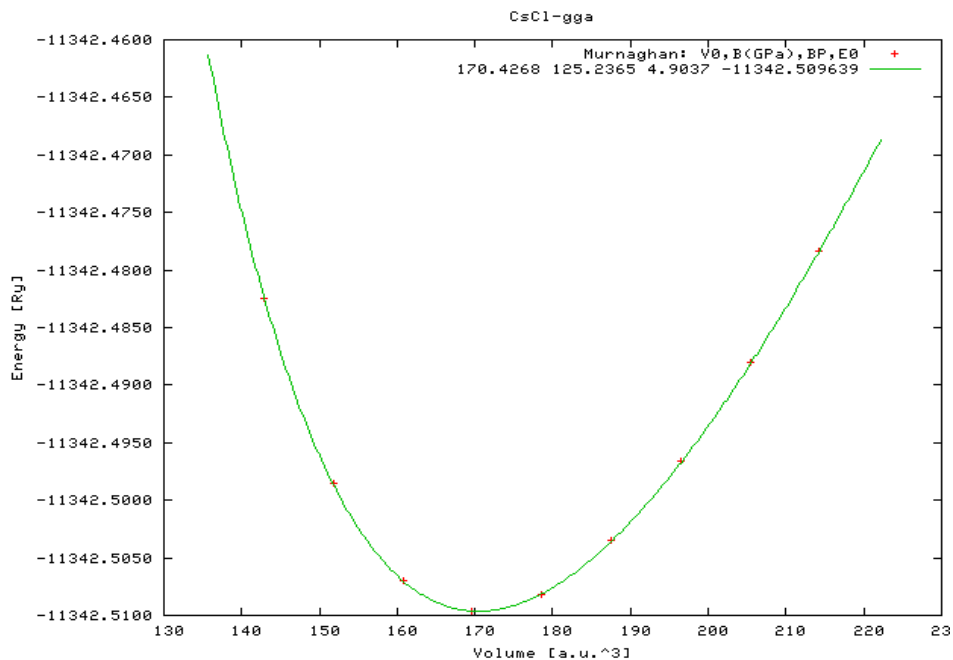
Table 4.1 Structural parameters of CdO in RS structure.

Phase	Method	a. (Å)			V.(a.u) ³	B (Gpa)		B'	E(Ry)
		present	Other calc	Exp		Present	Other calc		
RS	LDA	4.64			168.1533	160.5225	130 ^b	4.8885	-11331.64228
	GGA	4.77			183.3737	124.1466		4.8599	-11342.56863
	W-Cohen	4.70	4.77 ^a	4.697 ^c	174.6057	146.2835	130.5 ^c	4.8601	-11340.92803
			4.779 ^b						

^a Reference [48], ^b Reference [12], ^c Reference [49].

4.2.1.2 CsCl structure for CdO compound

The position of Cd is (0, 0, 0) a and the position of O is (0.5, 0.5, 0.5) a
 $R_{mt} = 2.05$ a.u for Cd and $R_{mt} = 1.75$ a.u for O. The suitable Rkmax of CsCl structure was found to be 8 for LDA and W-Cohen methods, and it was 8.5 for GGA method. The suitable k-point is 4500 with reduced $k_{point} = 120$ in the irreducible Brillouin zone. The Brillouin zone integrations were performed with a 16x16x16 K-mesh. G_{max} was 16 for GGA, but it was 15 for W-Cohen and 14 for LDA.

**Figure 4.2** Energy versus volume for CdO in CsCl structure with GGA method.

From Figure 4.2, energy versus volume we found V , B , B' , and E . Also we found the lattice parameters $a = b = c$ from

$$V = a^3 \quad (4.3)$$

Then

$$a = [V]^{1/3} \quad (4.4)$$

Table(4.2) shows the structural parameters in CsCl structure.

Table 4.2 Structural parameters of CdO in CsCl structure.

Phase	Method	a.(Å)		V.(a.u) ³	B (Gpa)		B'	E(Ry)
		Present	Other calc	Present	Present	Other calc	Present	Present
CsCl	LDA	2.85		155.4991	168.0635		4.9646	-11331.58665
	GGA	2.93		170.4088	127.2875		4.8596	-11342.50854
	W-Cohen	2.88		161.7786	151.1457		114 ^a	4.9794

^a Reference [48].

4.2.1.3 Zincblende structure for CdO compound

The position of Cd is $(0, 0, 0)a$ and the position of O is $(0.25, 0.25, 0.25)a$
 $R_{mt} = 2.05$ a.u for Cd and $R_{mt} = 1.75$ a.u for O, The suitable R_{kmax} of ZB structure was found to be 8 for LDA and W-Cohen, and it was 8.5 for GGA. The suitable k-point is 4500 with reduced $k_{point} = 120$ in the irreducible Brillouin zone. The Brillouin zone integrations were performed with a $16 \times 16 \times 16$ K-mesh. G_{max} was 16 for GGA, but it was 15 for W-Cohen and 14 for LDA.

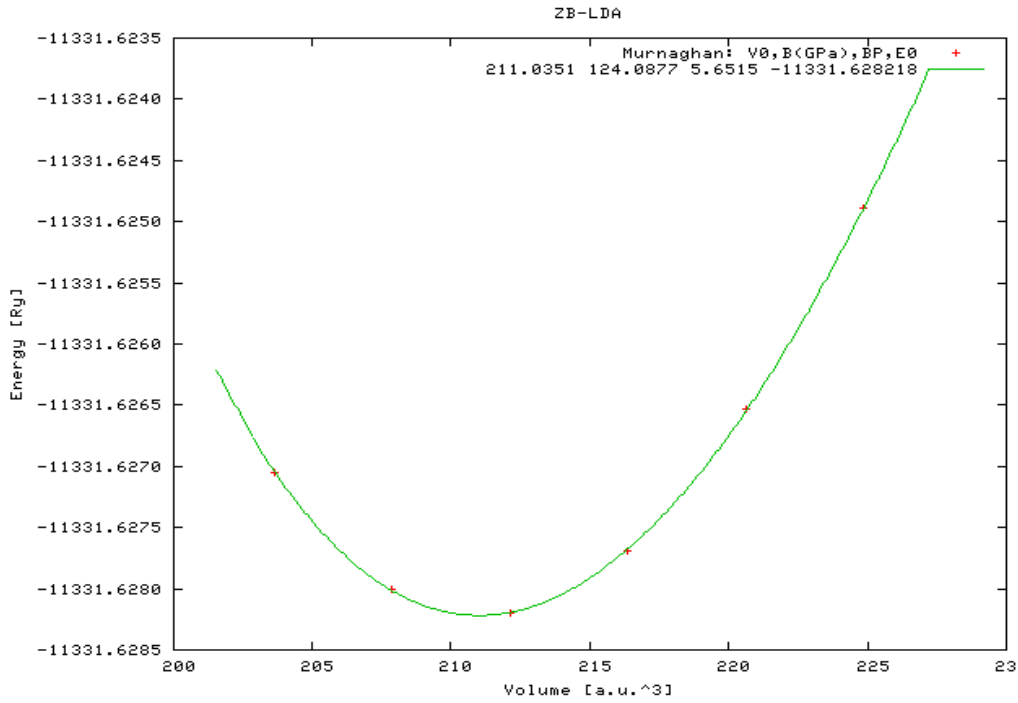


Figure 4.3 Energy versus volume for CdO in ZB structure with LDA method.

From Figure 4.3, energy versus volume we found V , B , B' , and E . Also we found the lattice parameters $a = b = c$ from

$$V = \frac{a^3}{4} \quad (4.5)$$

Then the lattice parameters

$$a = [4V]^{1/3} \quad (4.6)$$

Table 4.3 shows the structural parameters in ZB structure.

Table 4.3 Structural parameters of CdO in ZB structure.

Phase	Method	a. (Å)		V.(a.u) ³	B (Gpa)		B'	E(Ry)
		present	Other calc	present	Present	Other calc	Present	Present
ZB	LDA	5.0	5.15 ^a 5.148 ^b	211.1032	121.9463	82 ^a 93.9 ^b	5.1376	-11331.62805
	GGA	5.15		230.055	93.2264		4.7268	-11342.56546
	W-Cohen	5.07	219.4097	108.7127	5.064	-11340.91622		

^a Reference [48] , ^b Reference [12] .

4.2.1.4 Wurtzite structure for CdO compound

We chose the values of a , b , c and the ratio of c/a as arbitrary numbers and the angles $\alpha = \beta = 90$ and $\gamma = 120$, $R_{mt} = 2.05$ a.u for Cd and $R_{mt} = 1.75$ a.u for O. The suitable R_{kmax} of W structure is 8 for LDA and W-Cohen, and it was 8.5 for GGA. The suitable k -point is 6000 with reduced $k_{point} = 624$ in the irreducible Brillouin zone. The Brillouin zone integrations were performed with a $22 \times 22 \times 21$ K-mesh. G_{max} is 16 for GGA, but it was 15 for W-Cohen and 14 for LDA. The position of Cd is $(\frac{1}{3}, \frac{2}{3}, 0)a$ and the position of O is $(\frac{1}{3}, \frac{2}{3}, u)a$. Tables 4.4, 4.5 and 4.6 show the minimum energy for this work.

Table 4.4 Finding u of CdO by GGA method.

No.	U	E_{total} (Ry)	No.	U	E_{total} (Ry)
1	0.325	-22658.060941	10	0.370	-22685.130542
2	0.330	-22658.077081	11	0.375	-22685.131529
3	0.335	-22685.089822	12	0.380	-22685.131592
4	0.340	-22685.100399	13	0.385	-22685.131664
5	0.345	-22685.109463	14	0.390	-22685.131339
6	0.350	-22685.116263	15	0.395	-22685.094358
7	0.355	22685.122002	16	0.400	-22685.075637
8	0.360	-22685.125906	17	0.405	-22685.063765
9	0.365	-22685.128260	18	0.410	-22685.060110

Table 4.5 Finding u of CdO by W-Cohen method.

No.	U	E_{total} (Ry)	No.	U	E_{total} (Ry)
1	0.325	-22681.778429	10	0.370	-22681.830827
2	0.330	-22681.785471	11	0.375	-22681.831685
3	0.335	-22681.796586	12	0.380	-22681.831976
4	0.340	-22681.802805	13	0.385	-22681.832018
5	0.345	-22681.811450	14	0.390	-22681.831772
6	0.350	-22681.817605	15	0.395	-22681.831440
7	0.355	22681.823192	16	0.400	-22681.830791
8	0.360	-22681.826692	17	0.405	-22681.828658
9	0.365	-22681.829209	18	0.410	-22681.826438

Table 4.6 Finding u of CdO by LDA method.

No.	U	E_{total} (Ry)	No.	U	E_{total} (Ry)
1	0.325	-22663.179791	10	0.370	-22663.246811
2	0.330	-22663.195376	11	0.375	-22663.248015
3	0.335	-22663.206847	12	0.380	-22663.248198
4	0.340	-22663.216738	13	0.385	-22663.248365
5	0.345	-22663.225705	14	0.390	-22663.247470
6	0.350	-22663.231705	15	0.395	-22663.247133
7	0.355	22663.237808	16	0.400	-22663.246029
8	0.360	-22663.241474	15	0.405	-22663.243875
9	0.365	-22663.245961	16	0.410	-22663.242102

The minimum energy was found to be (-22685.131664 Ry) as shown in table 4.4, which means the correct value for u is (0.385). Then by fitting the results with Murnaghan's equation of states and plotting the energy versus volume graph, we found the minimum volume V , bulk modulus B , first derivative of the bulk modulus B' and minimum energy E . Then we found the values a , c , c/a . Tables 4.7, 4.8 and 4.9 show these values.

Table 4.7 Finding c/a of CdO in GGA method.

no.	Value	a=b (a.u)	C (a.u)	c/a	E_{total} (Ry)
1	-10	6.67710	10.68434	1.6001	-22685.112597
2	-5	6.79915	10.87864	1.6000	-22685.127097
3	0	6.91640	11.06624	1.6000	-22685.119973
4	5	7.02980	11.24769	1.6000	-22685.131634
5	10	7.13966	11.42346	1.6000	-22685.128614

Table 4.8 Finding c/a of CdO in W-Cohen method.

no.	Value	a=b (a.u)	c (a.u)	c/a	E_{total} (Ry)
1	-10	6.67710	10.68434	1.6001	-22681.835066
2	-5	6.79915	10.87864	1.6000	-22681.828639
3	0	6.91640	11.06624	1.6000	-22681.834967
4	5	7.02980	11.24769	1.6000	-22681.807174
5	10	7.13966	11.42346	1.6000	-22681.831986

Table 4.9 Finding c/a of CdO in LDA method.

no.	Value	a=b (a.u)	C (a.u)	c/a	E _{total} (Ry)
1	-10	6.67710	10.68434	1.6001	-22663.285352
2	-5	6.79915	10.87864	1.6000	-22663.257605
3	0	6.91640	11.06624	1.6000	-22663.212371
4	5	7.02980	11.24769	1.6000	-22663.248357
5	10	7.13966	11.42346	1.6000	-22663.232678

Then fitting these data in Fortran program called polyfit to get the best value for c/a by GGA, GDA and W-Cohen methods, we found this value is (c/a=1.60), then from the graph of energy versus volume we found V, B, B', and E. Also we found the lattice parameters a, b, c from

The volume of the unit cell for wurtzite is

$$V = \frac{\sqrt{3}}{2} a^2 c \quad (4.7)$$

by rewriting this equation

$$V = \frac{\sqrt{3}}{2} a^3 (c/a) \quad (4.8)$$

then

$$a = \left[\frac{2V}{\sqrt{3}(c/a)} \right]^{1/3} \quad (4.9)$$

By substituting the volume (V) from the graph of energy versus volume and c/a from the table in equation (4.9), we can find the value of a, b and c exactly. The last step we used the new values of a, b, c and u to find the band gap, by doing a new optimizing job. Table 4.10 shows these values.

Table 4.10 Structural parameters of CdO in wurtzite structure.

parameter	Present calculations			Other calculations
	LDA	GGA	W-Cohen	
a(Å)	3.5607	3.6634	3.6063	3.66 ^a , 3.678 ^b
c(Å)	5.697	5.86	5.77	5.865 ^a , 5.825 ^b
c/a	1.6	1.6	1.6	1.6 ^a , 1.58 ^b
U	0.385	0.385	0.385	0.35 ^a , 0.3849 ^b
V.(a.u) ³	422.1589	459.4927	438.57	
B(Gpa)	180.81	94.27	108.63	86 ^a , 92.7 ^b
B'	4.924	4.62	4.91	4.52 ^a , 4.7 ^b
E(RY)	-22663.3	-22685.2	-22681.8	

^a Reference [48] , ^b Reference [12].

4.2.2 Band structure for CdO compound

The studying of band structures and calculating the energy band gaps are very important for any material to determine whether this material is metal, semiconductor or insulator.

Figures 4.4 to 4.7 show the band structure for CdO in all its structures.

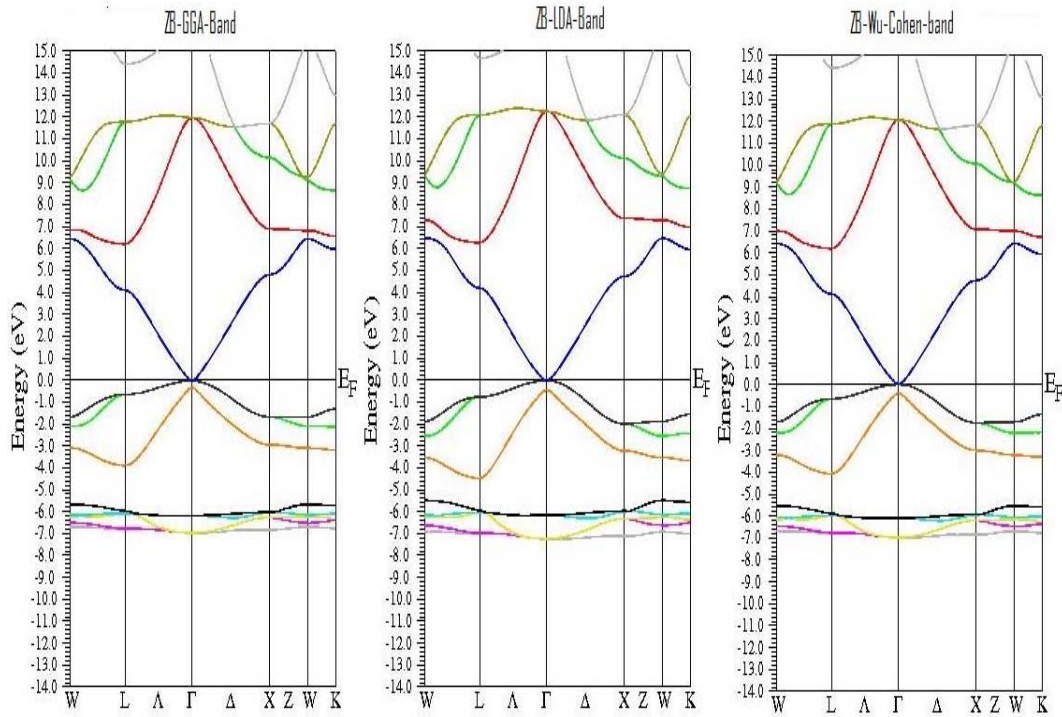


Figure 4.4 Band structure of CdO in ZB with (from left to right) GGA , LDA and W-Cohen methods respectively.

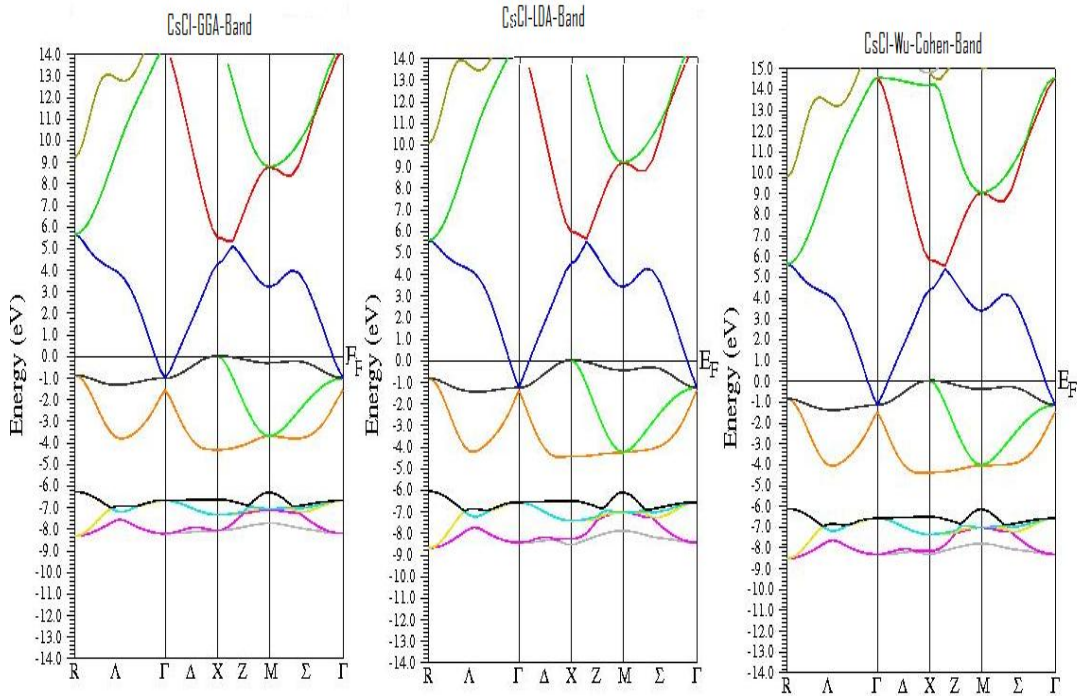


Figure 4.5 Band structure of CdO in CsCl with (from left to right) GGA , LDA and W-Cohen methods respectively.

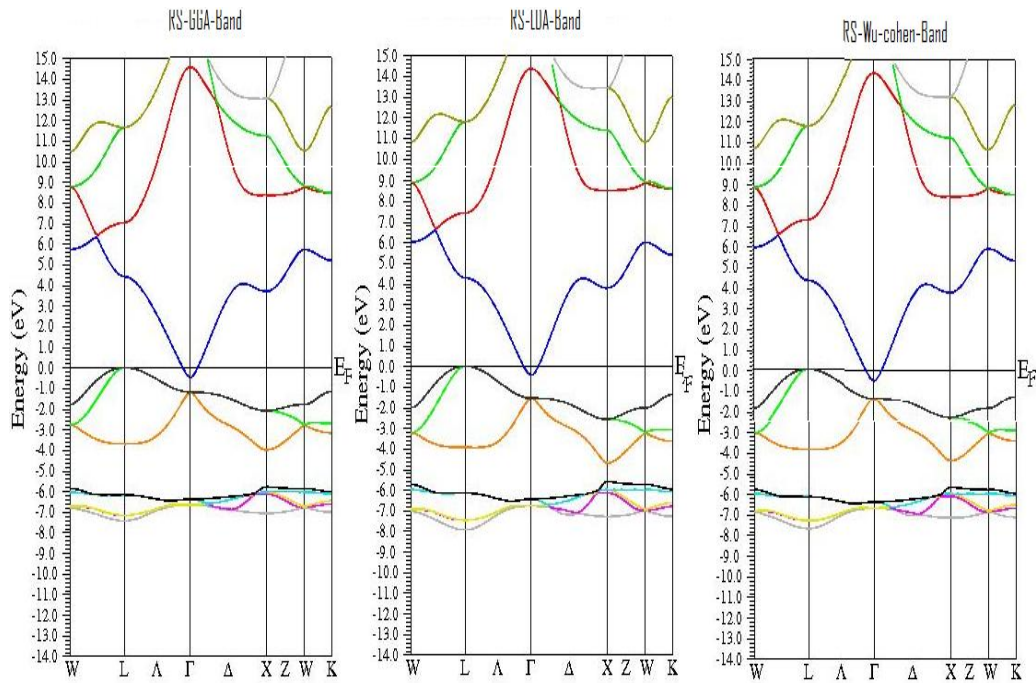


Figure 4.6 Band structure of CdO in RS with (from left to right) GGA , LDA and W-Cohen methods respectively.

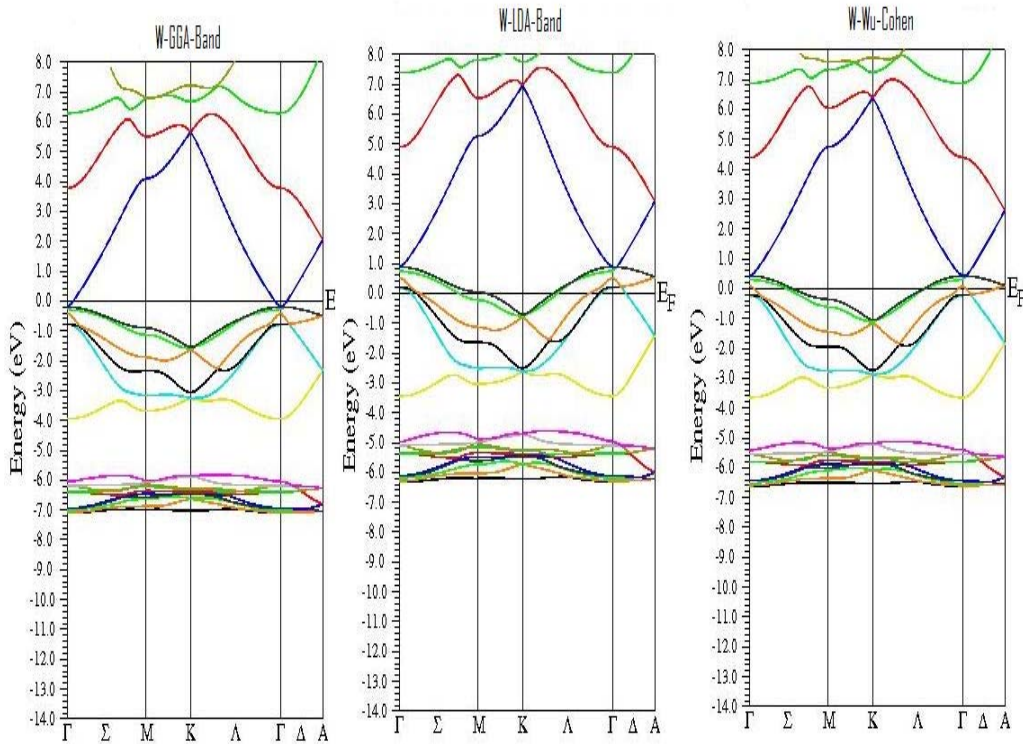


Figure 4.7 Band structure of CdO in Wurtzite with (from left to right) GGA , LDA and W-Cohen methods respectively.

The energy band gap for rocksalt was found to be - 0.50047 eV, - 0.44788 eV and - 0.52308 eV for GGA, LDA and W-Cohen respectively, but for Cesium chloride the energy gap was found to be -1.03891 eV, -1.28324 eV and -1.18536 eV for GGA, LDA and W-Cohen respectively, therefore the band structure indicates a semimetal. For Zincblende the energy gap was found to be 0.17466 eV for GGA, 0.12668 eV for LDA and 0.18937eV for W-Cohen respectively. Finally for wurtzite structure the energy gap was found to be 0.13684 eV for GGA, 0.13872 eV for LDA and 0.11352 eV for W-Cohen respectively. But other calculation was found to be 0.66 eV. Table 4.11 shows the energy band gap of all structures studied in this thesis.

Table 4.11 The energy band gap of CdO in RS, CsCl, ZB and WZ structures.

Structure	Method	energy band gap(eV)	
		Present	Other calculation
RS	GGA	-0.50047	0.66 ^a
	LDA	-0.44788	
	W-Cohen	-0.52308	
CsCl	GGA	-1.03891	
	LDA	-1.28324	
	W-Cohen	-1.18536	
ZB	GGA	0.17466	
	LDA	0.12668	
	W-Cohen	0.18937	
WZ	GGA	0.13684	
	LDA	0.13872	
	W-Cohen	0.11352	

^a Reference [12].

4.2.3 Phase transition pressure for CdO compound

The lattice parameters should change from a structure to another under certain pressure which is called transition pressure (P_t). We can find the value of this pressure from graph energy versus volume for the two phases. By making a line

which has same tangent for both curves, then the slope of the tangent represents the transition pressure (P_t) as follows:

$$P_t = -\frac{\Delta E}{\Delta V} \quad (4.10)$$

Then multiply the slope by the factor 14684.9761724 in order to get the transition pressure (P_t) in Gpa.

Figure 4.8 shows the EO'S for both RS & CsCl structures using GGA method. The transition pressure was found to be 51.5 Gpa.

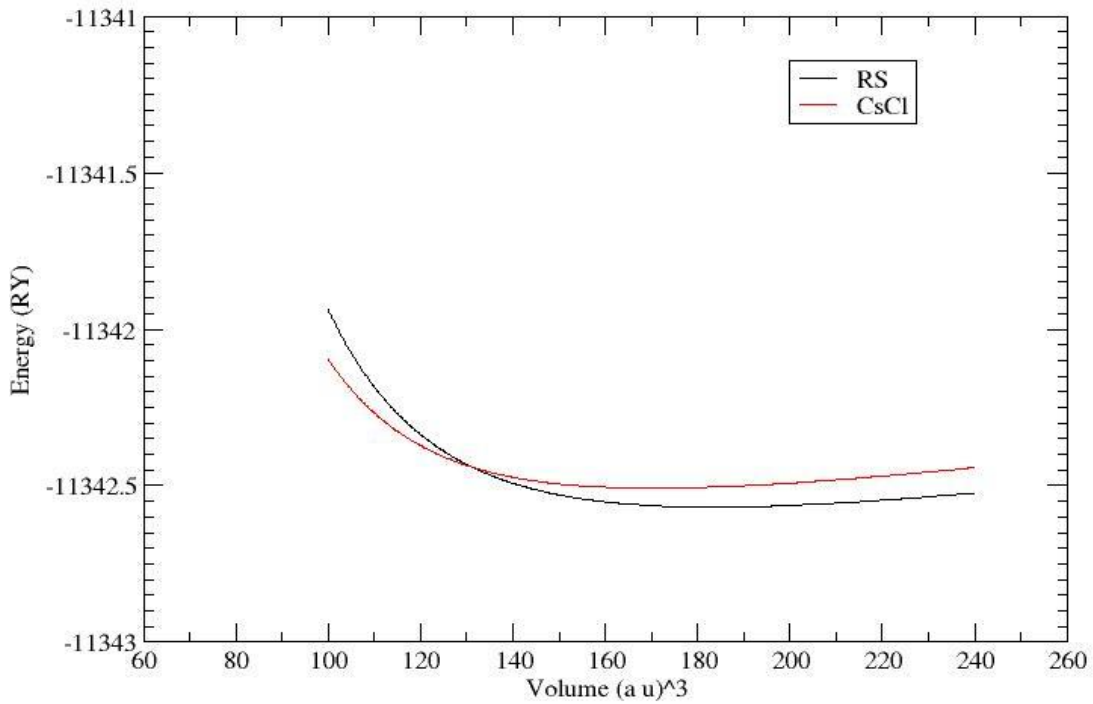


Figure 4.8 Equations of state for CdO in RS and CsCl structures by GGA method.

Figure 4.9 shows the EO'S for both RS & CsCl structures using LDA method. The transition pressure was found to be 72.75 Gpa .

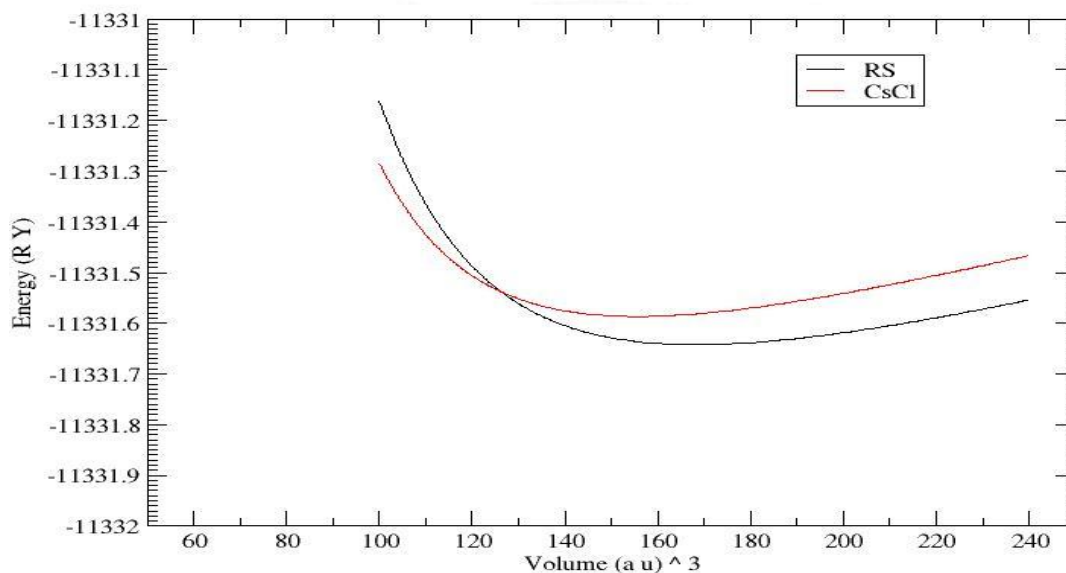


Figure 4.9 Equations of state for CdO in RS and CsCl structures by LDA method.

Figure 4.10 shows the EO'S for both RS & CsCl structures using W-Cohen method. The transition pressure was found to be 78.8 Gpa .

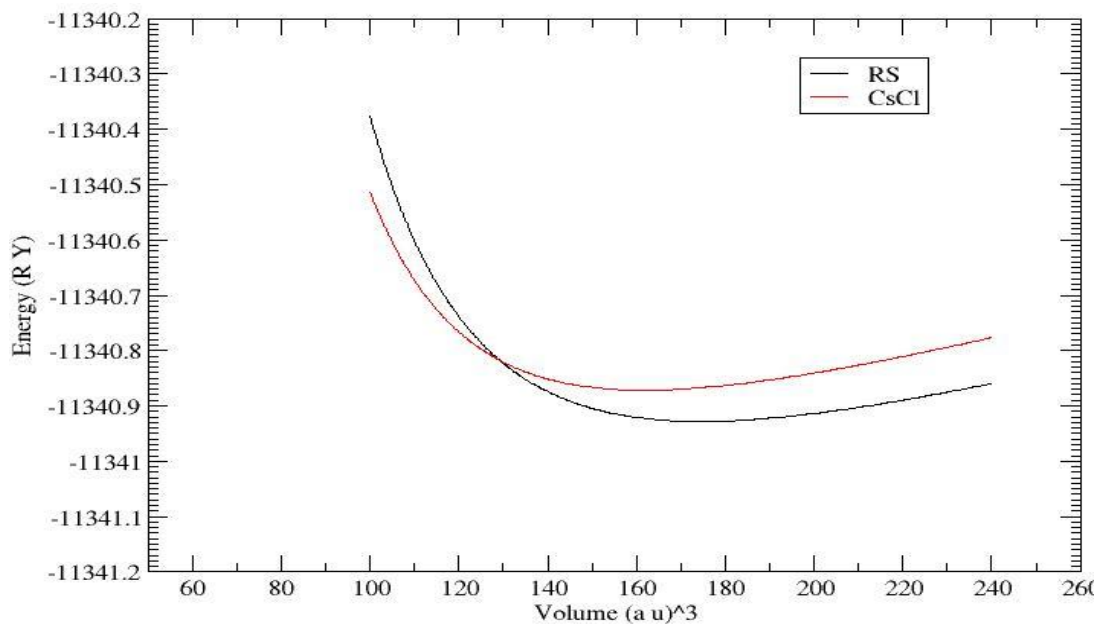


Figure 4.10 Equations of state for CdO in RS and CsCl structures by W-Cohen method.

Figure 4.11 shows the EO'S for both wurtzite & CsCl structures using GGA method. The transition pressure was found to be 12.46 Gpa .

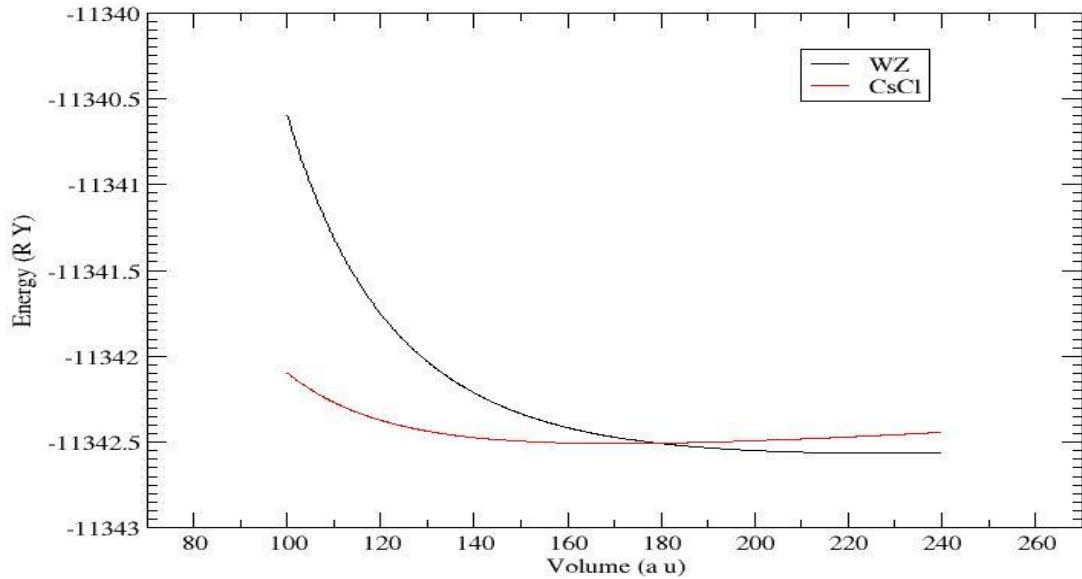


Figure 4.11 Equations of state for CdO in Wurtzite and CsCl structures by GGA method.

Figure 4.12 shows the EO'S for both wurtzite & CsCl structures using LDA method. The transition pressure was found to be 13.74 Gpa .

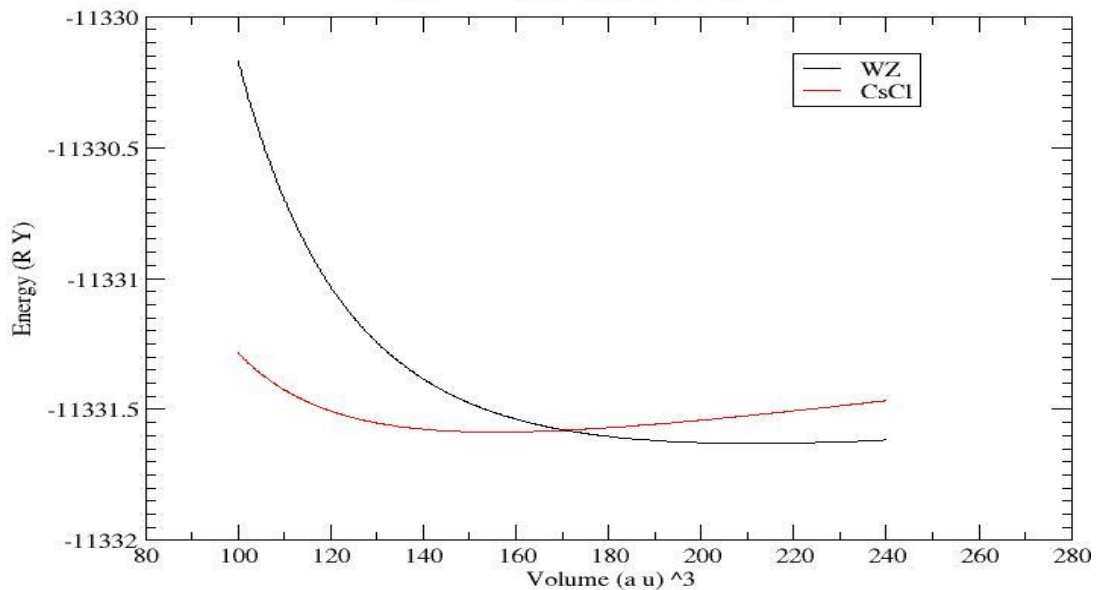


Figure 4.12 Equations of state for CdO in Wurtzite and CsCl structures by LDA method.

Figure 4.13 shows the EO'S for both wurtzite & CsCl structures using W-Cohen method. The transition pressure was found to be 15.87 Gpa .

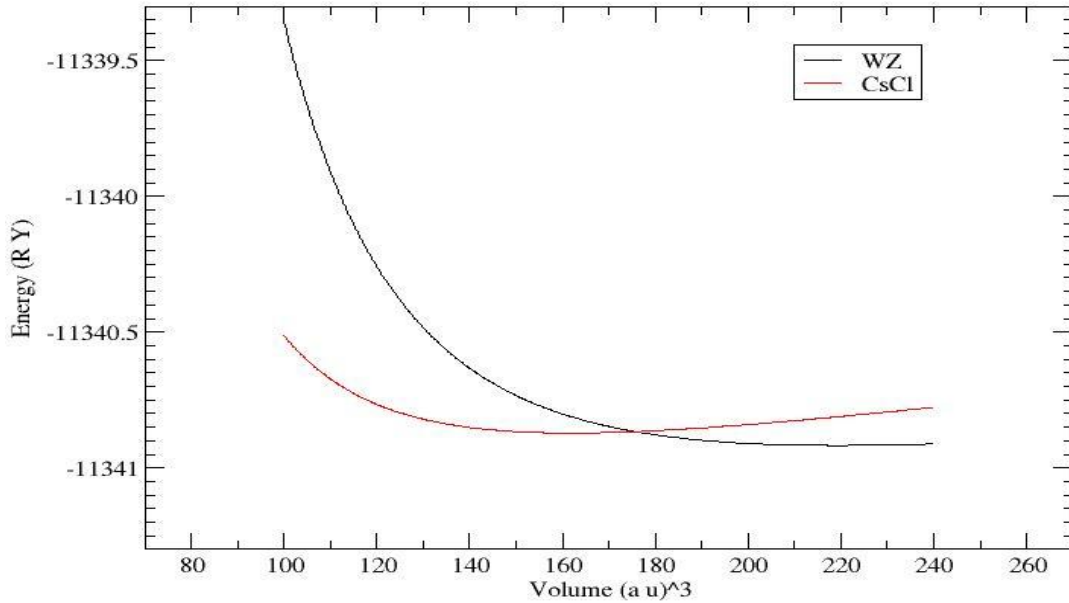


Figure 4.13 Equations of state for CdO in WZ and CsCl structures by W-Cohen method.

Figure 4.14 shows the EO'S for both ZB & CsCl structures using GGA method. The transition pressure was found to be 6.84 Gpa .

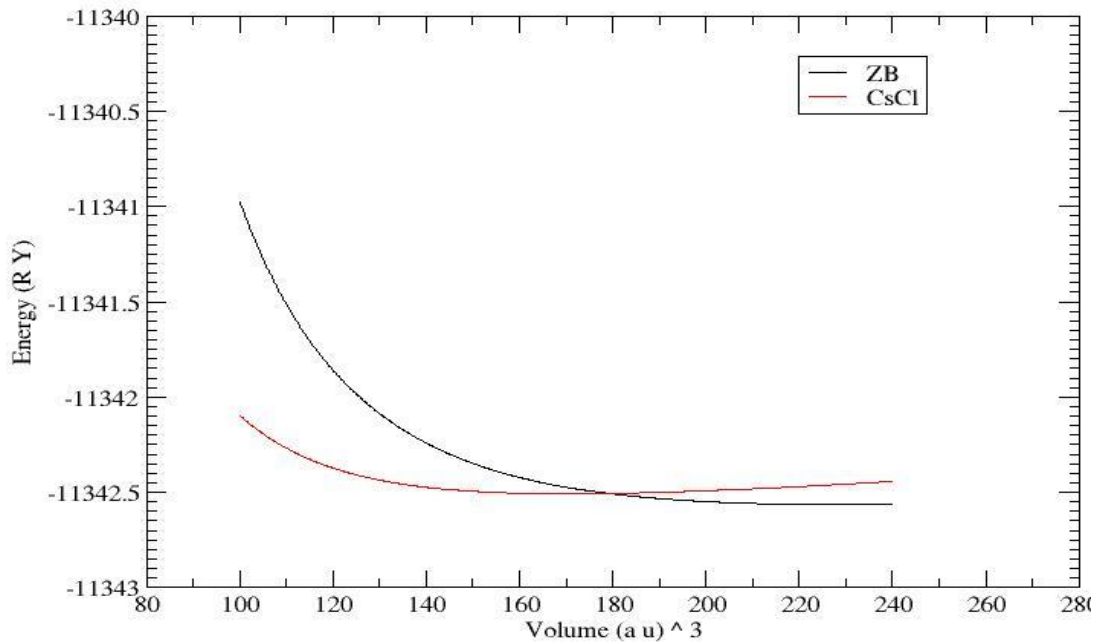


Figure 4.14 Equations of state for CdO in ZB and CsCl structures by GGA method.

Figure 4.15 shows the EO'S for both ZB & CsCl structures using LDA method. The transition pressure was found to be 2.5 Gpa .

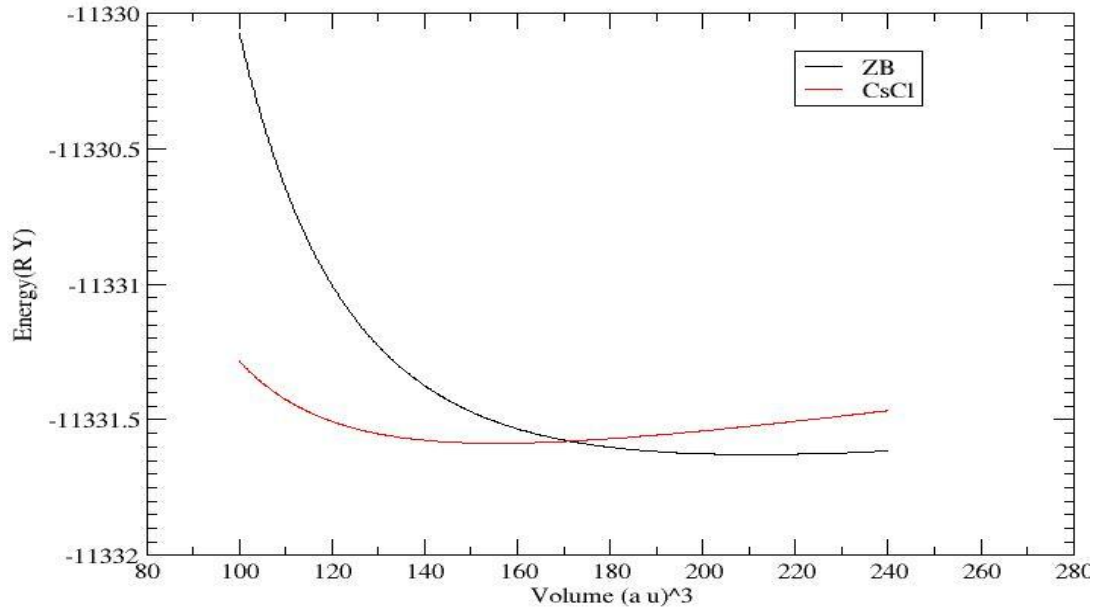


Figure 4.15 Equations of state for CdO in ZB and CsCl structures by LDA method.

Figure 4.16 shows the EO'S for both ZB & CsCl structures using W-Cohen method. The transition pressure was found to be 5.67 Gpa .

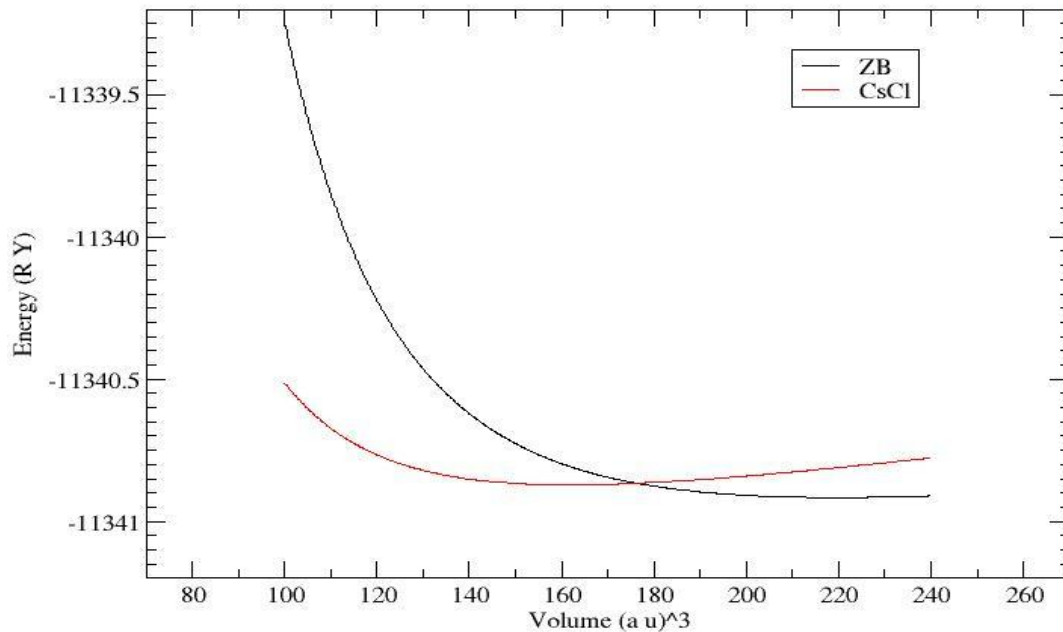


Figure 4.16 Equations of state for CdO in ZB and CsCl structures by W-Cohen method.

Transition from wurtzite to ZB couldn't be calculated as shown in figures 4.17, 4.18 and 4.19 since the curves laid over each other.

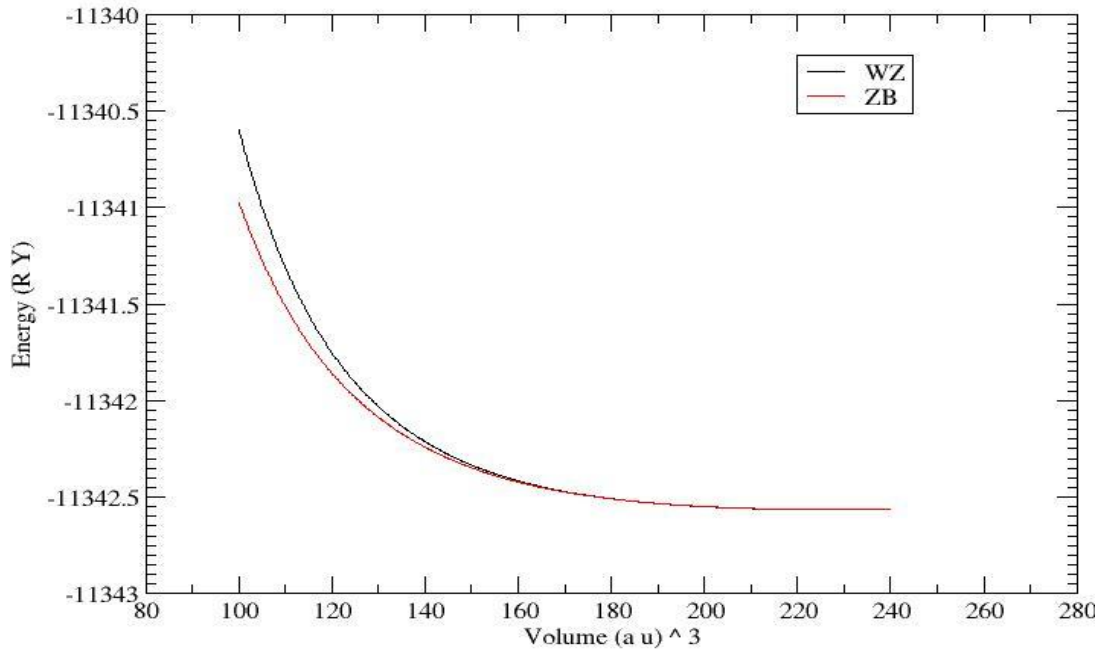


Figure 4.17 Equations of state for CdO in Wurtzite and ZB structures by GGA method.

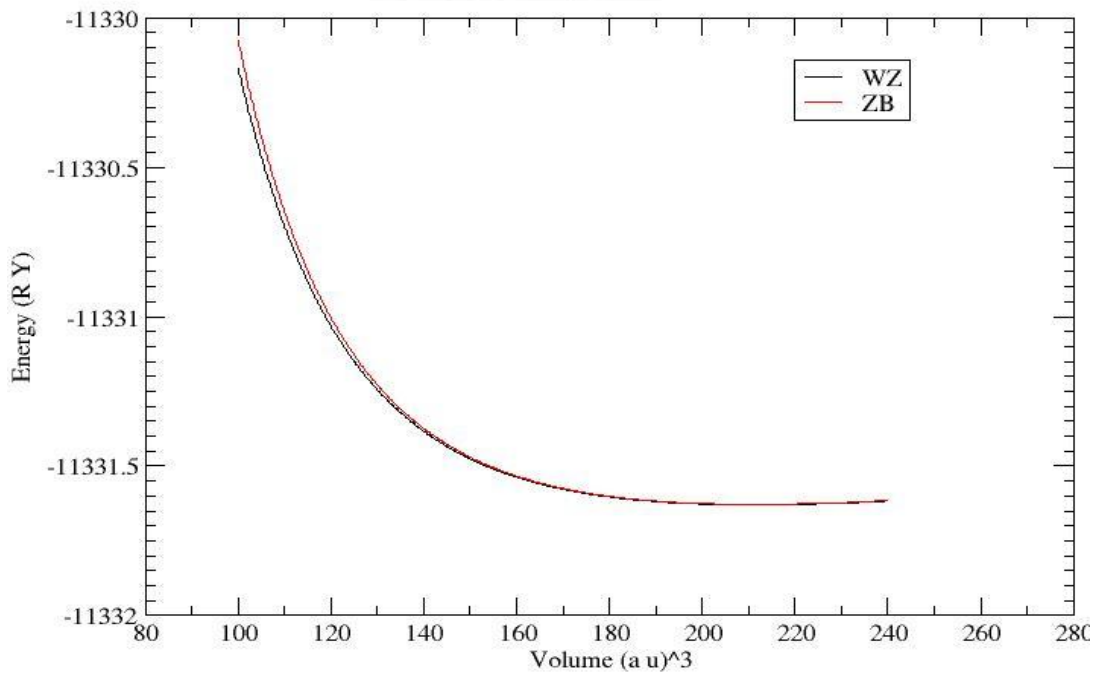


Figure 4.18 Equations of state for CdO in Wurtzite and ZB structures by LDA method.

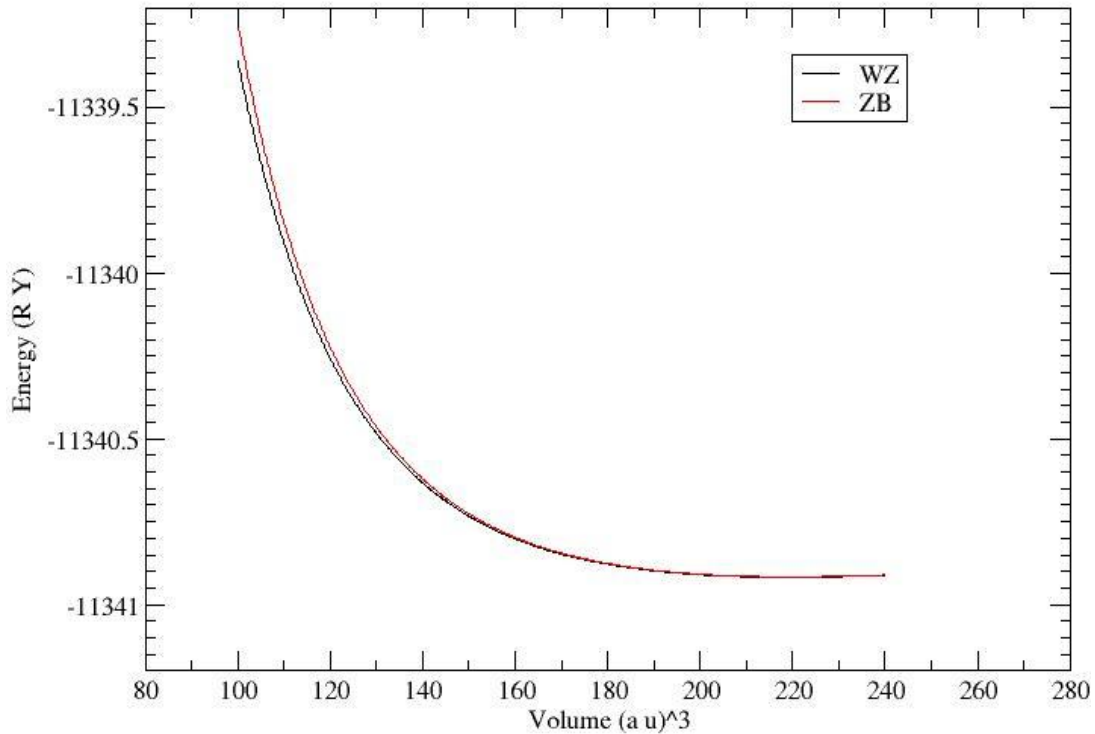


Figure 4.19 Equations of state for CdO in ZB and WZ structures by W-Cohen method.

Figures 4.20, 4.21 and 4.22 show the EO'S for both ZB & RS using GGA, LDA , W-Cohen methods respectively. Figures 4.23, 4.24 and 4.25 show the EO'S for both wurtzite & RS structures using GGA, LDA , W-Cohen methods respectively. It is very clear that the energy between any two phases in these figures is continuously diverge with increasing pressure, indicating a phase transformation from ZB to RS, and from wurtzite to CsCl is impossible under high pressure [50].

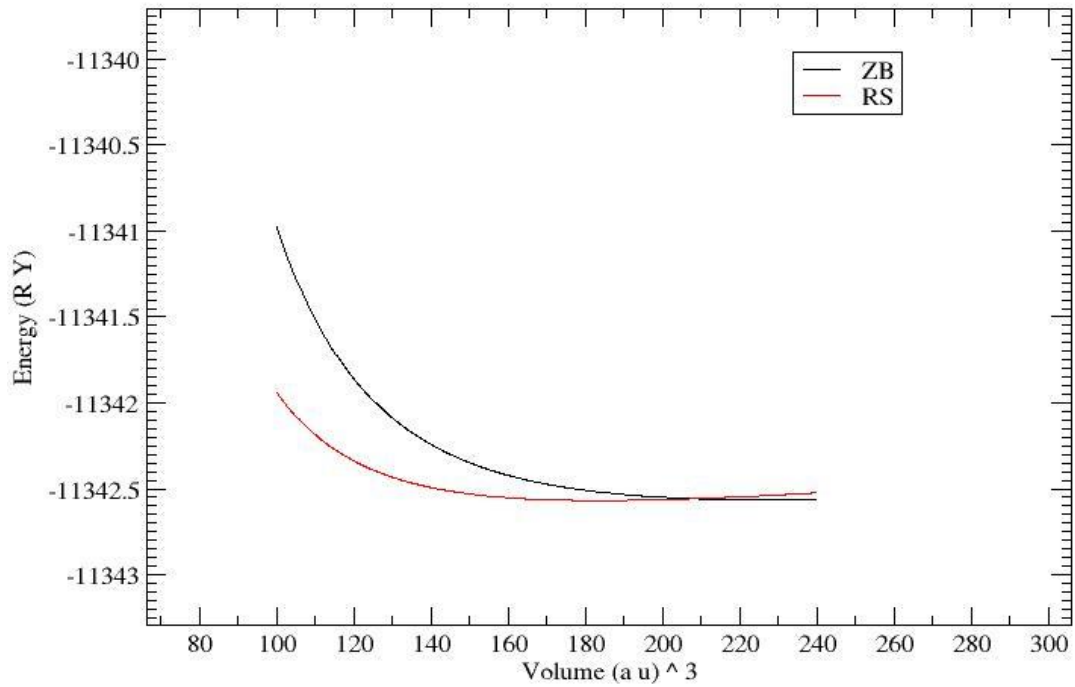


Figure 4.20 Equations of state for CdO in ZB and RS structures by GGA method.

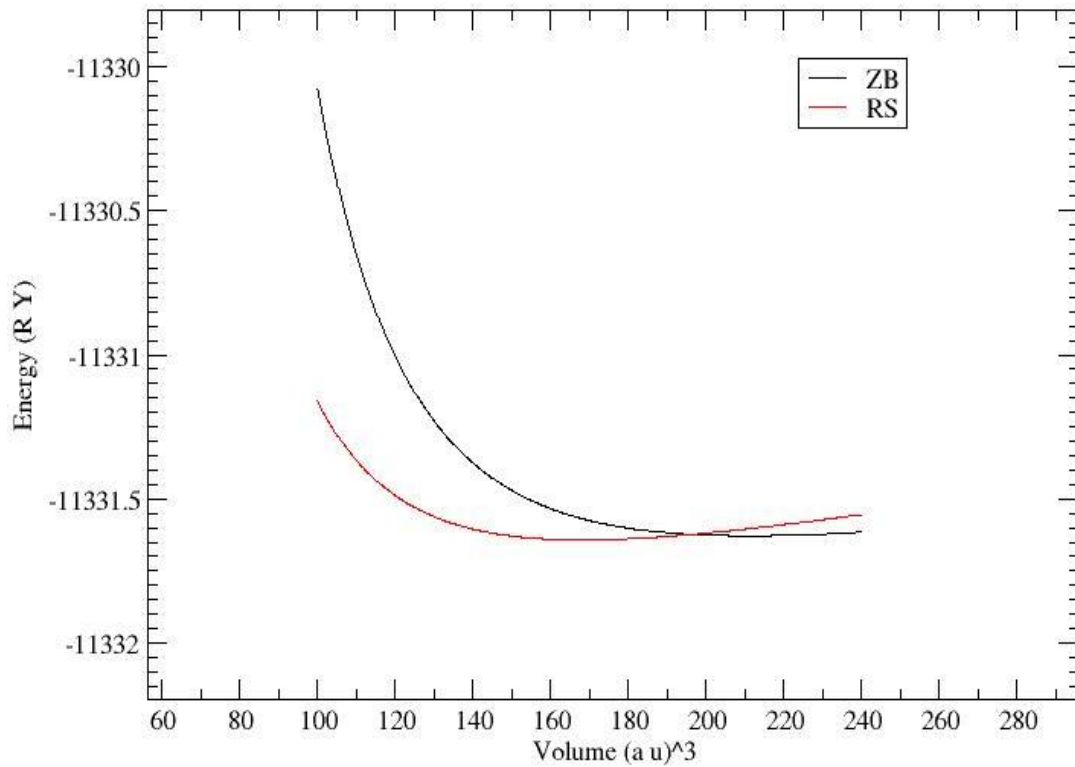


Figure 4.21 Equations of state for CdO in ZB and RS structures by LDA method.

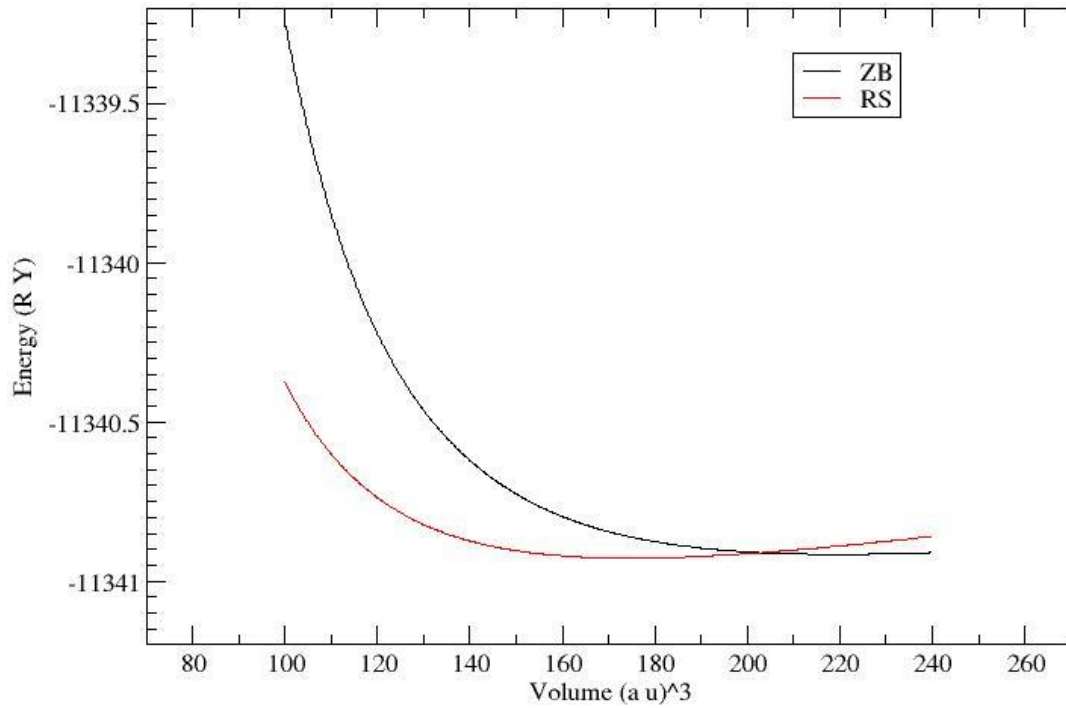


Figure 4.22 Equations of state for CdO in ZB and RS structures by W-Cohen method.

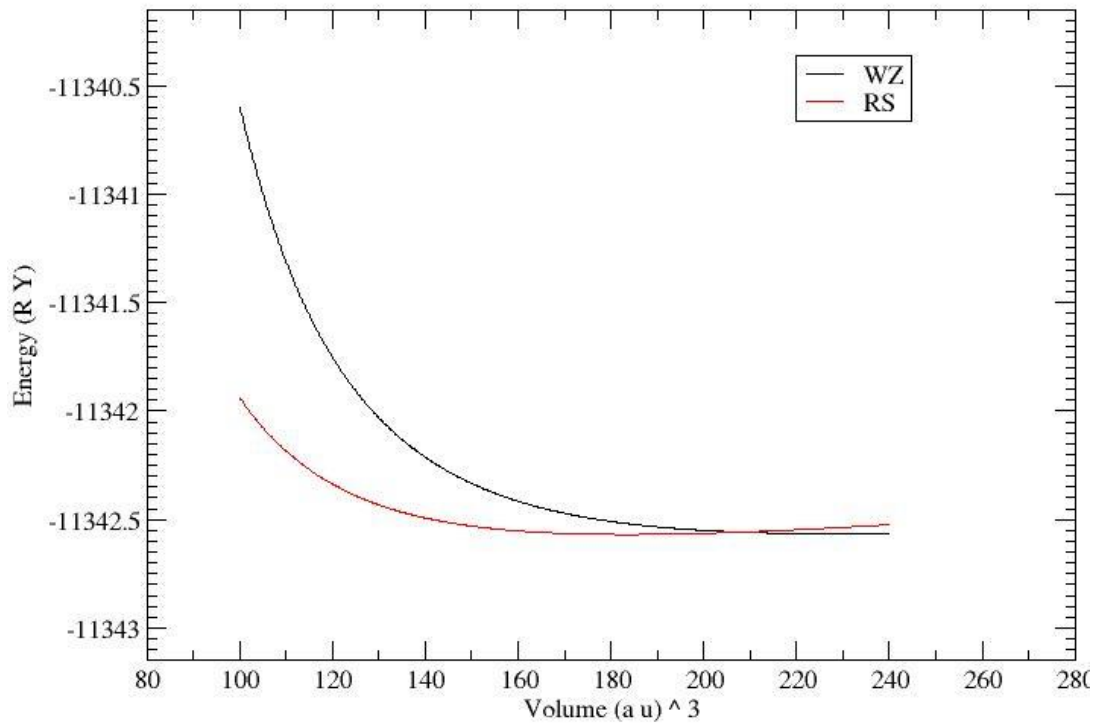


Figure 4.23 Equations of state for CdO in Wurtzite and RS structures by GGA method.

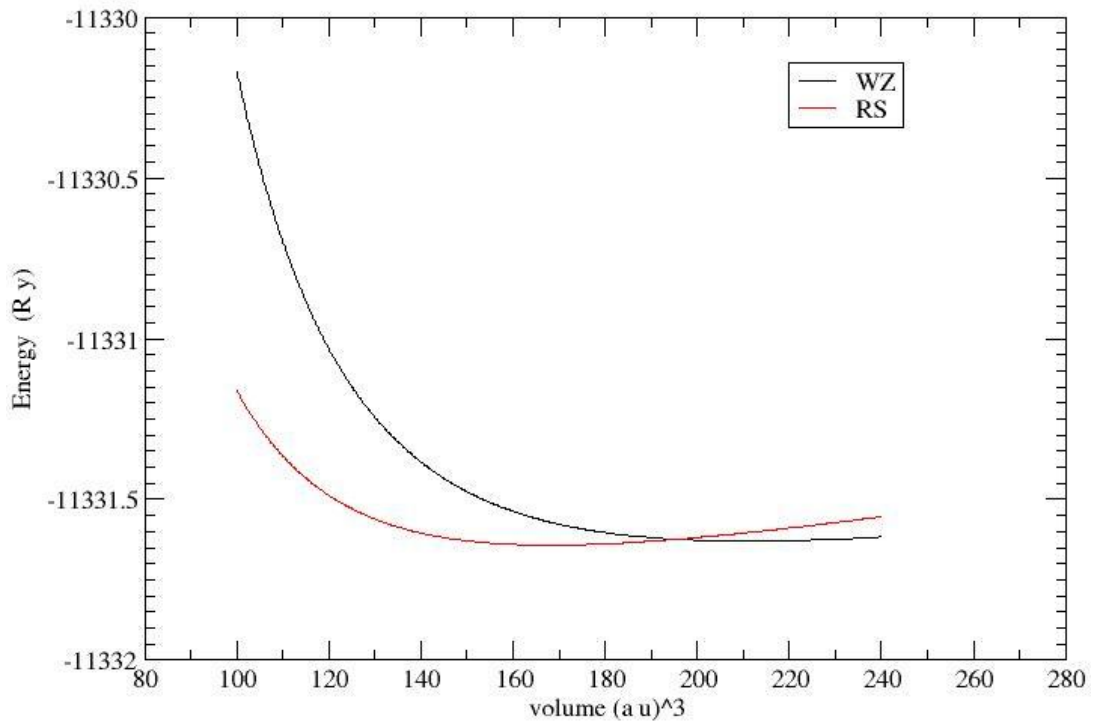


Figure 4.24 Equations of state for CdO in Wurtzite and RS structures by LDA method.

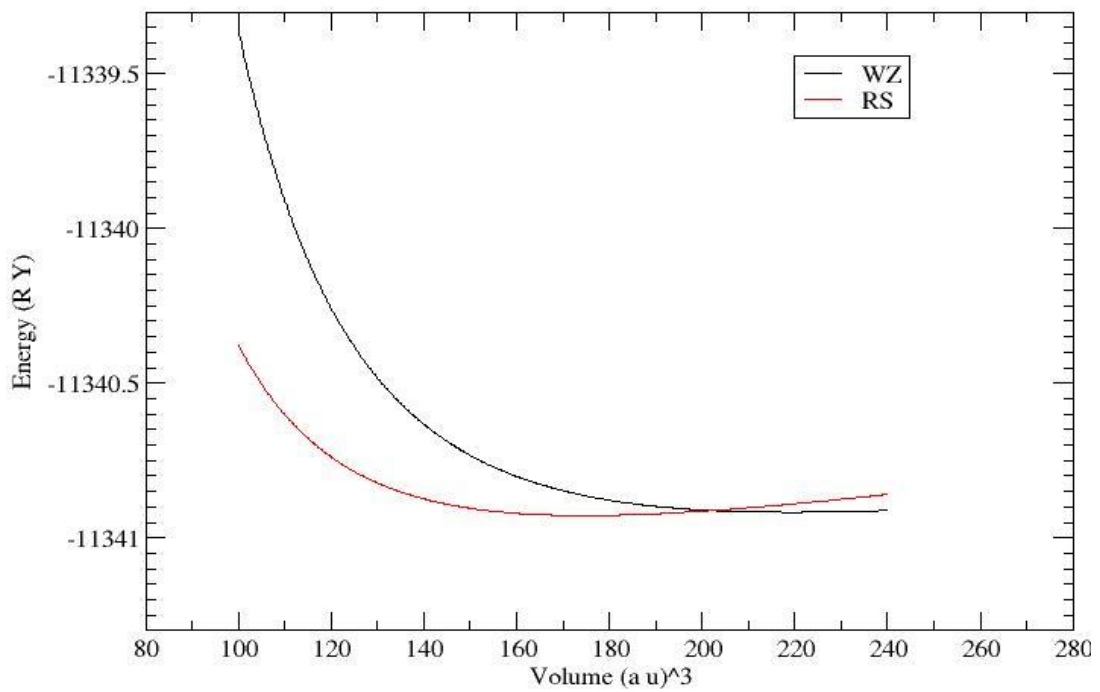


Figure 4.25 Equations of state for CdO in WZ and RS structures by W-Cohen method.

Figures 4.26, 4.27 and 4.28 show the four structures together on laid on one graph using LDA, GGA and W-Cohen methods. These graphs also show RS structure is the ground state for CdO compound.

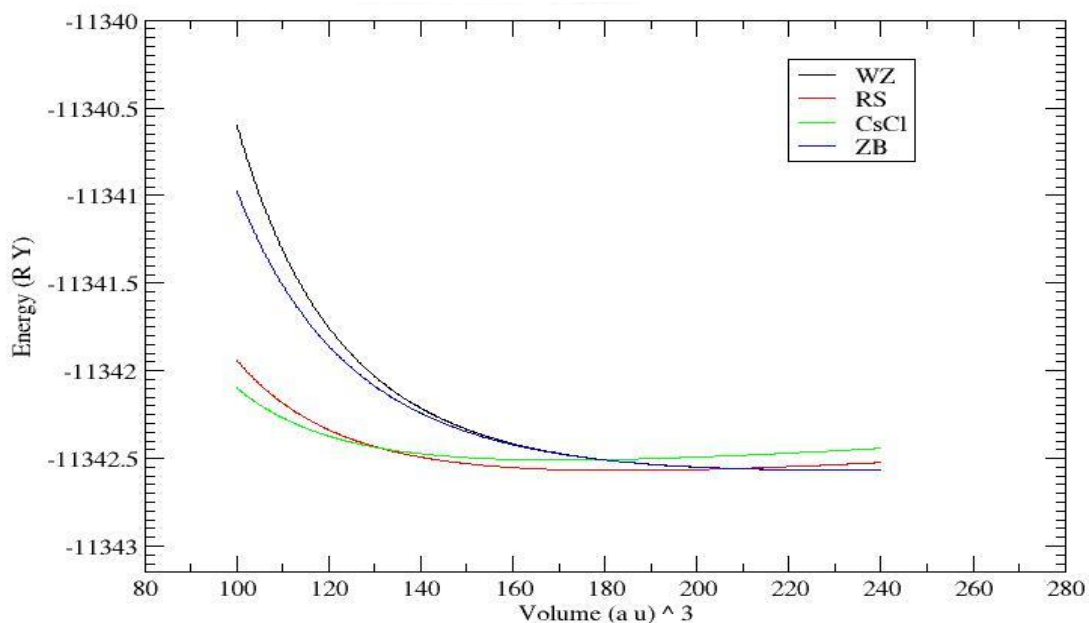


Figure 4.26 Equations of state for CdO in RS, CsCl, ZB and WZ structures by GGA method.

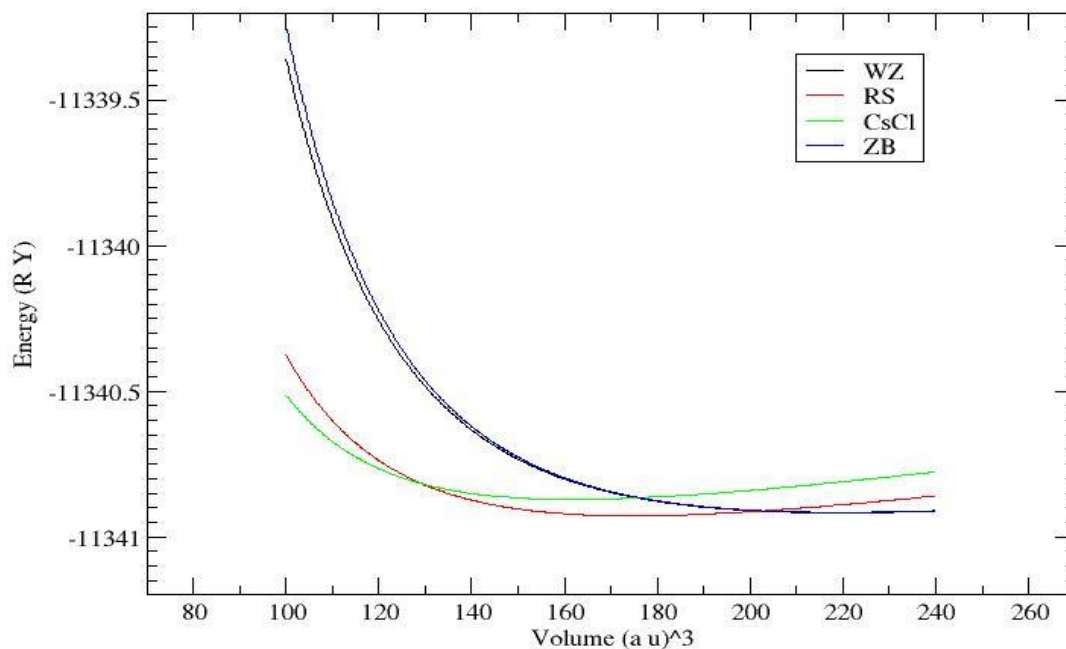


Figure 4.27 Equations of state for CdO in RS, CsCl, ZB and WZ structures by W-Cohen method.

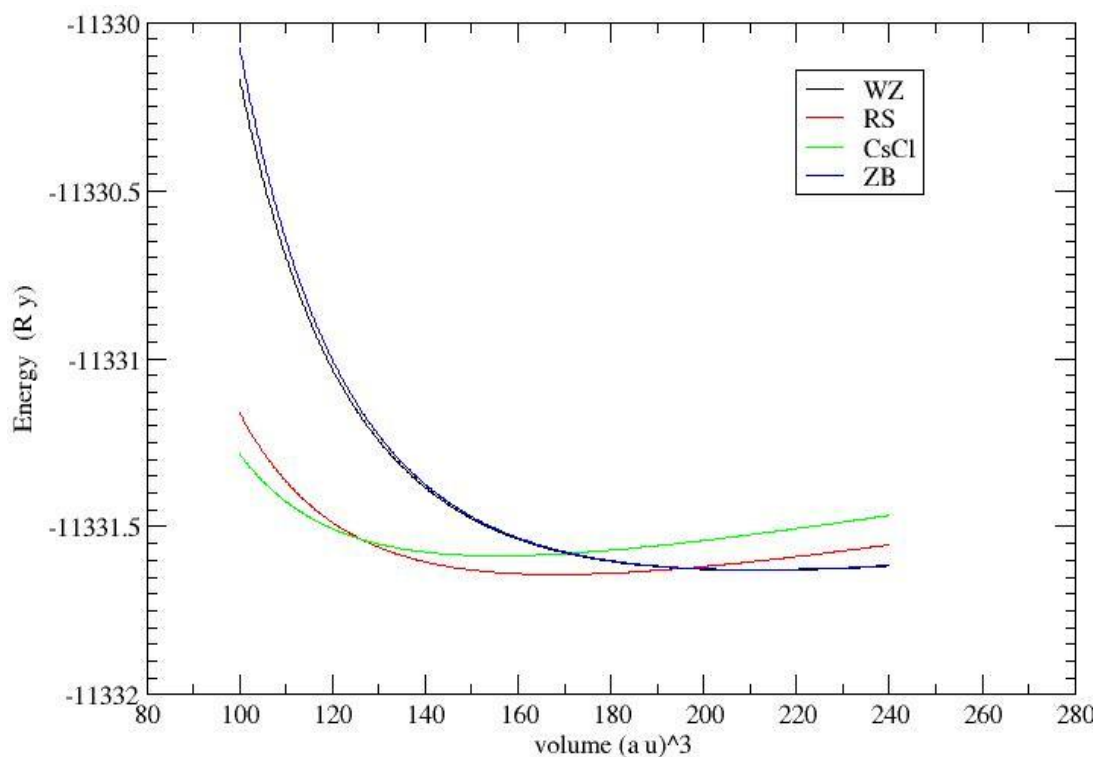


Figure 4.28 Equations of state for CdO in RS, CsCl, ZB and WZ structures by LDA method.

Table 4.12 shows the value of the transition pressure between the phases of CdO compound.

Table 4.12 The transition pressure between RS, CsCl, ZB and WZ structures for CdO.

Transition	Studied parameter	Present calculations			Exp	Other calc
		LDA	GGA	W-Cohen		
RS-CsCl	Pt(Gpa)	72.57	51.5	78.82	90.6 ^a	89 ^b , 81.7 ^c
WZ-CsCl	Pt(Gpa)	13.74	12.46	15.87		
WZ-RS	Pt(Gpa)	6.2	3.7	xxxxxx		
ZB-CsCl	Pt(Gpa)	2.5	6.84	5.67		
ZB-RS	Pt(Gpa)	1.85	7.7	xxxxxx		
ZB-WZ	Pt(Gpa)	xxxxxxx	xxxxxxx	xxxxxx		

^a Reference [14], ^b Reference [48], ^c Reference [51].

4.3 CoO compound

As we did for CdO compound we also did for CoO compound. We studied its structural phases, Rocksalt (RS), Cesium Chloride (CsCl) and Zincblende (ZB). We calculated the structural parameters and the energy band gaps for each phase by using the FP-LAPW approach depending on the density functional theory using GGA, LDA and W-Cohen methods. We also studied the transition pressure between its phases, from RS to CsCl, ZB to CsCl, and from ZB to RS structures. Also we investigated the stability of its ground state.

4.3.1 Structural parameters for CoO compound

We calculated the structural parameters of CoO in its state RS, CsCl and ZB by using FP-LAPW in GGA, LDA, and W-Cohen methods. We obtained these structural parameters a , b , c , B and B' for CoO structures, from Energy versus volume graph.

4.3.1.1 Rocksalt structure for CoO compound

We found the structural parameters for CoO in RS structure by GGA, LDA, and W-Cohen. The position of Co is $(0, 0, 0)a$ and the position of O is $(0.5, 0.5, 0.5)a$. R_{mt} is the atomic sphere radius (muffin-tin-radius) for atoms under study. The WIEN2k code can set this R_{mt} automatically, $R_{mt} = 2.05$ a.u for Cd and $R_{mt} = 1.75$ a.u for O. K_{max} is the maximum value for the K vector in the reciprocal lattice, and R is the average value of the R_{mt} for all atomic spheres, Tables from 4.13 to 4.16 show the tests done to choose RK_{max} and Kpoints for RS CsCl and ZB structures, where the best values for RK_{max} and Kpoints which have the minimum energy. From table 4.13 and table 4.14 we found that the best

RK_{\max} was found to be 8 for LDA and W-Cohen, and 8.5 for GGA, but the suitable k points is 3000 with 84 reduced K_{points} in the irreducible Brillouin zone. The Brillouin zone integrations were performed with a $14 \times 14 \times 14$ K-mesh. G_{\max} was 16 for GGA, but it was 15 for W-Cohen and 14 for LDA. Table 4.17 shows the structural parameters in RS structure.

Table 4.13 Test to find RK_{\max} for RS, CsCl and ZB structures.

Rkmax test for CsCl by LDA			Rkmax test for ZB by W-Cohen			Rkmax test for RS by GGA		
method			method			method		
no	Rkmax	Etotal (Ry)	No	Rkmax	Etotal (Ry)	No	RKmax	Etotal (Ry)
1	6	-2931.708736	1	6	-2936.305738	1	6	-2937.294677
2	6.5	-2931.714871	2	6.5	-2936.310663	2	7	-2937.302249
3	7	-2931.726534	3	7	-2936.315833	3	7.5	-2937.314771
4	7.7	-2931.735255	4	7.5	-2936.327593	4	8	-2937.321839
5	8	-2931.744189	5	8	-2936.336551	5	8.5	-2937.333026
6	8.5	-2931.735223	6	8.5	-2936.327472	6	9	-2937.327451
7	9	-2931.728645	7	9	-2936.316401	7	9.5	-2937.313279
8	9.5	-2931.721987	8	9.5	-2936.310859	8	10	-2937.302755
			9	10	-2936.302493			

Table 4.14 Choosing the best k_{points} for CsCl structure by GGA method.

No	K_{points}	K_{reduced}	Matrix	Etotal (Ry)
1	2000	56	$12 \times 12 \times 12$	-2937.302095
2	2500	84	$13 \times 13 \times 13$	-2937.302147
3	3000	84	$14 \times 14 \times 14$	-2937.302247
4	3500	120	$15 \times 15 \times 15$	-2937.302200
5	4500	120	$16 \times 16 \times 16$	-2937.302141
6	6500	165	$18 \times 18 \times 18$	-2937.301296
7	8500	220	$20 \times 20 \times 20$	-2937.302085
8	9500	286	$21 \times 21 \times 21$	-2937.302187
9	12500	364	$23 \times 23 \times 23$	-2937.302044

Table 4.15 Choosing the best k_{points} for RS structure by LDA method.

No	K_{points}	Kreduced	Matrix	Etotal (Ry)
1	2000	56	12×12×12	-2931.841312
2	2500	84	13×13×13	-2931.841374
3	3000	84	14×14×14	-2931.841419
4	3500	120	15×15×15	-2931.841386
5	4500	120	16×16×16	-2931.841326
6	6500	165	18×18×18	-2931.841343
7	8500	220	20×20×20	-2931.841286
8	9500	286	21×21×21	-2931.841223
9	12500	364	23×23×23	-2931.841207

Table 4.16 Choosing the best k_{points} for ZB structure by W-Cohen method.

No	K_{points}	Kreduced	Matrix	Etotal (Ry)
1	2000	56	12×12×12	-2936.308155
2	2500	84	13×13×13	-2936.308143
3	3000	84	14×14×14	-2936.308187
4	3500	120	15×15×15	-2936.308137
5	4500	120	16×16×16	-2936.308107
6	6500	165	18×18×18	-2936.308143
7	8500	220	20×20×20	-2936.307985
8	9500	286	21×21×21	-2936.308111
9	12500	364	23×23×23	-2936.307967

Table 4.17 Structural parameters of CoO in RS structure by GGA, LDA and W-Cohen approximations.

Phase	Method	a.(Å)			V.(a.u) ³	B (Gpa)		B'	E.(Ry)
		Present	Other calc	Exp		Present	Other calc		
RS	LDA	4.034	4.11 ^a	4.254 ^b	110.7171	369.0392	250 ^a	7.6723	-2931.837385
	GGA	4.123			118.2647	230.8117		5.2089	-2937.373399
	W-Cohen	4.073			114.0237	300.921		6.6579	-2936.34284

^a Reference [52],^b Reference [53].

4.3.1.2 CsCl structure for CoO compound

The position of Co is (0, 0, 0)a and the position of O is (0.5, 0.5, 0.5) a
 $R_{mt} = 2.05$ a.u for Cd and $R_{mt} = 1.75$ a.u for O. The best RK_{max} was found to be 8 for LDA and W-Cohen, 8.5 for GGA, but the suitable kpoints is 3000 with 84 reduced K_{points} in the irreducible Brillouin zone. The Brillouin zone integrations were performed with a 14x14x14 K-mesh. G_{max} was 16 for GGA, but it was 15 for W-Cohen and 14 for LDA. Table 4.18 shows the structural parameters in CsCl structure.

Table 4.18 Structural parameters of CoO in CsCl structure by GGA, LDA and W-Cohen approximations.

Phase	method	a.(Å)	V.(a.u) ³	B (Gpa)	B'	E.(Ry)
		Present	Present	Present	Present	Present
CsCl	LDA	2.5	105.0849	326.2657	5.1247	-2931.787457
	GGA	2.562	113.4866	248.6075	4.8377	-2937.313853
	W-Cohen	2.53	109.0469	297.9795	4.6296	-2936.28824

4.3.1.3 Zincblende structure for CoO compound

The position of Co is (0, 0, 0)a and the position of O is (0.25, 0.25, 0.25)a
 $R_{mt} = 2.05$ a.u for Cd and $R_{mt} = 1.75$ a.u for O. The best RK_{max} was found to be 8 for LDA and W-Cohen, 8.5 for GGA, and the suitable kpoints is 3000 with 84 reduced K_{points} in the irreducible Brillouin zone. The Brillouin zone integrations were performed with a 14x14x14 K-mesh. G_{max} was 16 for GGA, but it was 15 for W-Cohen and 14 for LDA. Table 4.19 shows the structural parameters in ZB structure.

Table 4.19 Structural parameters of CoO in ZB structure by GGA, LDA and W-Cohen approximations.

Phase	method	a.(Å)	V.(a.u) ³	B (Gpa)	B'	E.(Ry)
		Present	Present	Present	Present	Present
ZB	LDA	4.32	136.0328	360.4126	9.2155	-2931.865184
	GGA	4.421	145.7941	286.6523	9.7195	-2937.401025
	W-Cohen	4.349	138.798	284.7843	7.9247	-2936.368621

4.3.2 The energy band gaps for CoO compound

The energy band gap for rocksalt was found to be 0.01122 eV for GGA, 0.42596 eV for LDA and 0.14552 eV for W-Cohen, but for Cesium chloride the energy gap was found to be 0.77975 eV for GGA, 1.0956 eV for LDA and 0.76518 eV for W-Cohen. Finally, for Zincblende the energy gap was found to be - 0.54942 eV for GGA, - 0.17252 eV for LDA and - 0.50409 eV for W-Cohen. But other calculation was found to be 2.5 eV. Table 4.20 shows the energy band gap for all structures.

Table 4.20 The energy band gaps for CoO in ZB, RS and CsCl structures.

Structure	Method	Energy band gap(eV)		
		Present	Other calculations	Experiment
ZB	GGA	-0.54942	0.0 ^a	2.5 ^c
	LDA	-0.17252		
	W-Cohen	-0.50409		
RS	GGA	0.01122		
	LDA	0.42596		
	W-Cohen	0.14552		
CsCl	GGA	0.77975	3.5 ^b	
	LDA	1.09560		
	W-Cohen	0.76518		

^a Reference [52],

^b Reference [54],

^c Reference [55].

Figures 4.29, 4.30 and 4.31 show the energy band structures for all CoO structures.

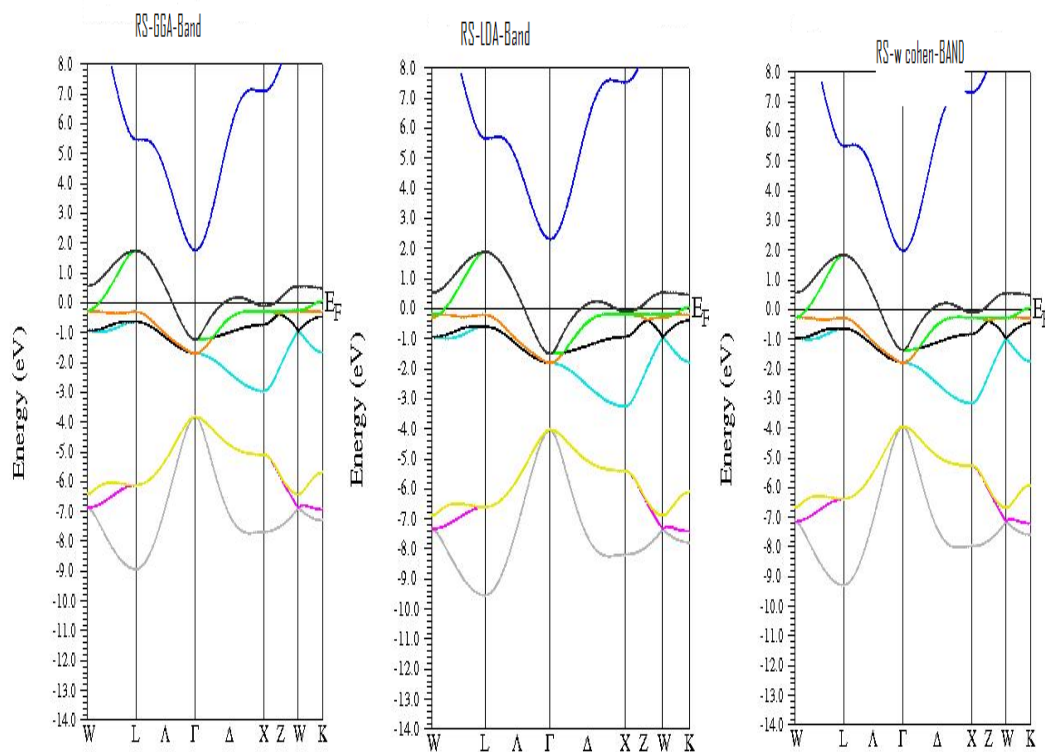


Figure 4.29 Band structure of CoO in RS with (from left to right) GGA , LDA and W-Cohen methods respectively.

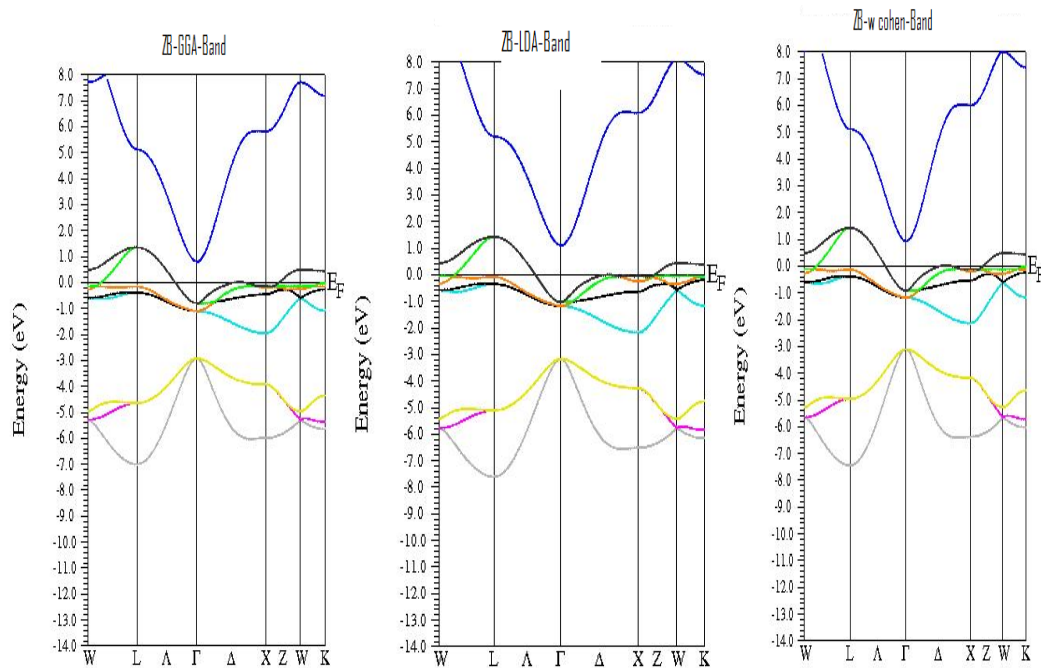


Figure 4.30 Band structure of CoO in ZB with (from left to right) GGA , LDA and W-Cohen methods respectively.

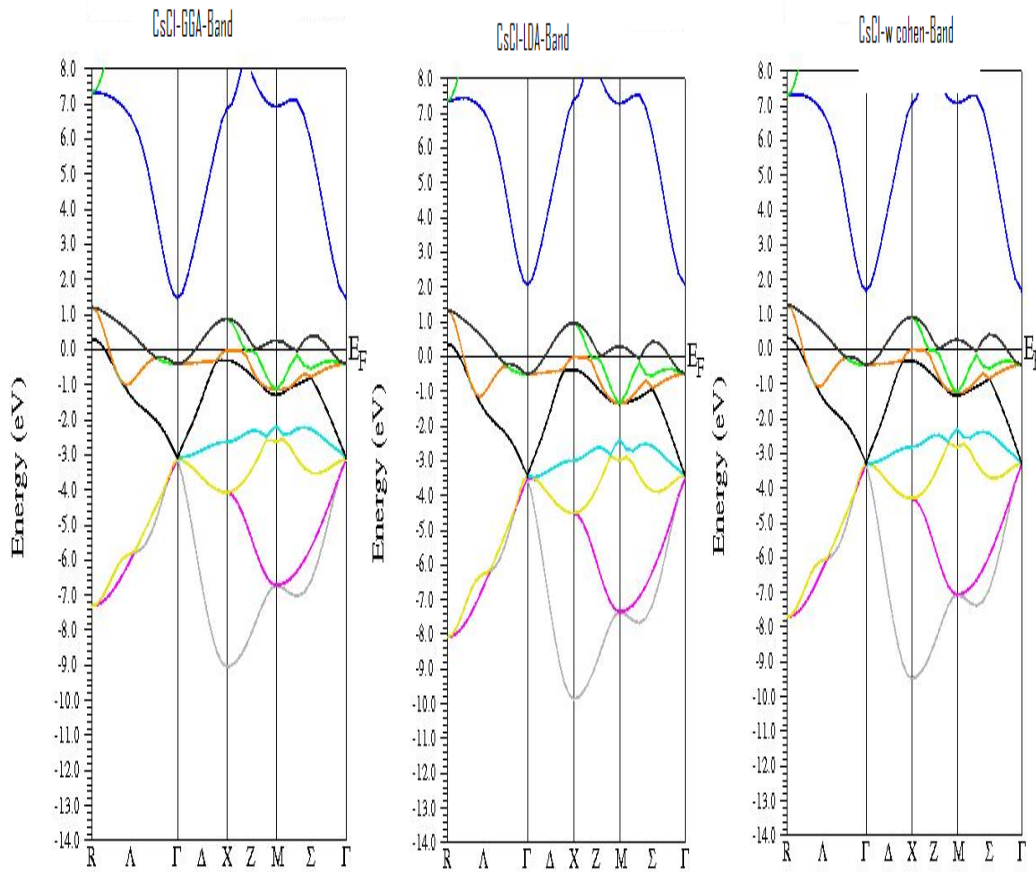


Figure 4.31 Band structure of CoO in CsCl with (from left to right) GGA , LDA and W-Cohen methods respectively.

4.3.3 Phase transition pressure for CoO compound

The same way which was done for the transition under high pressure for CdO compound we did for CoO compound.

Figure 4.32 shows the EO'S for both RS & CsCl structures using GGA method. The transition pressure was found to be 126.78 Gpa.

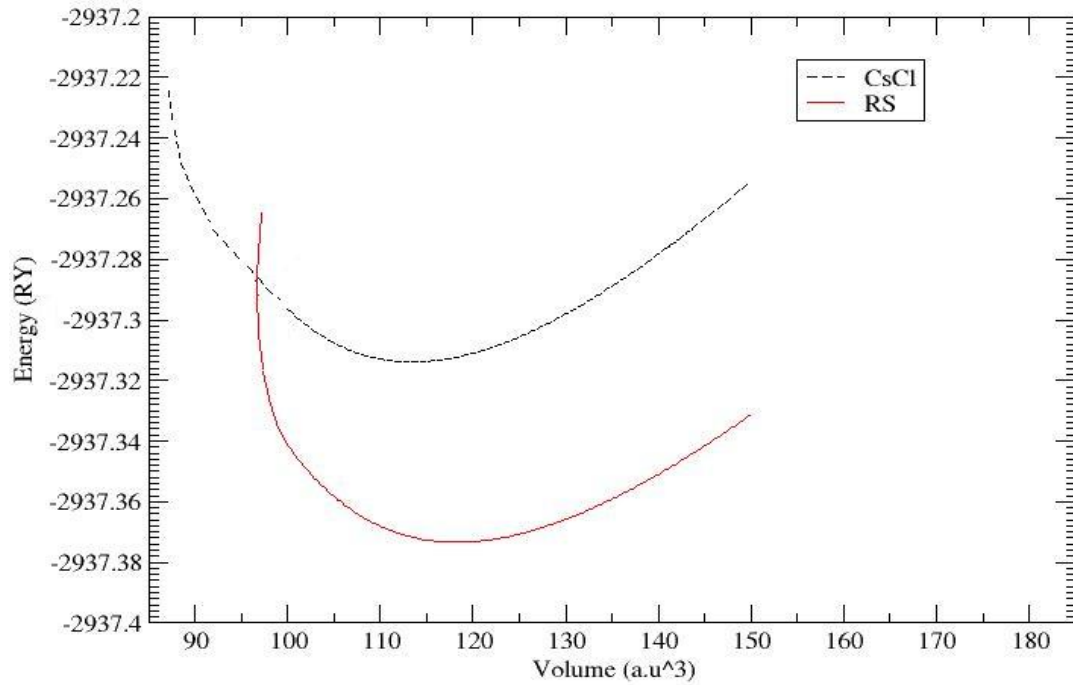


Figure 4.32 Equations of state for CoO in RS and CsCl structures by GGA method.

Figure 4.33 shows the EO'S for both RS & CsCl structures using LDA method. The transition pressure was found to be 104.206 Gpa .

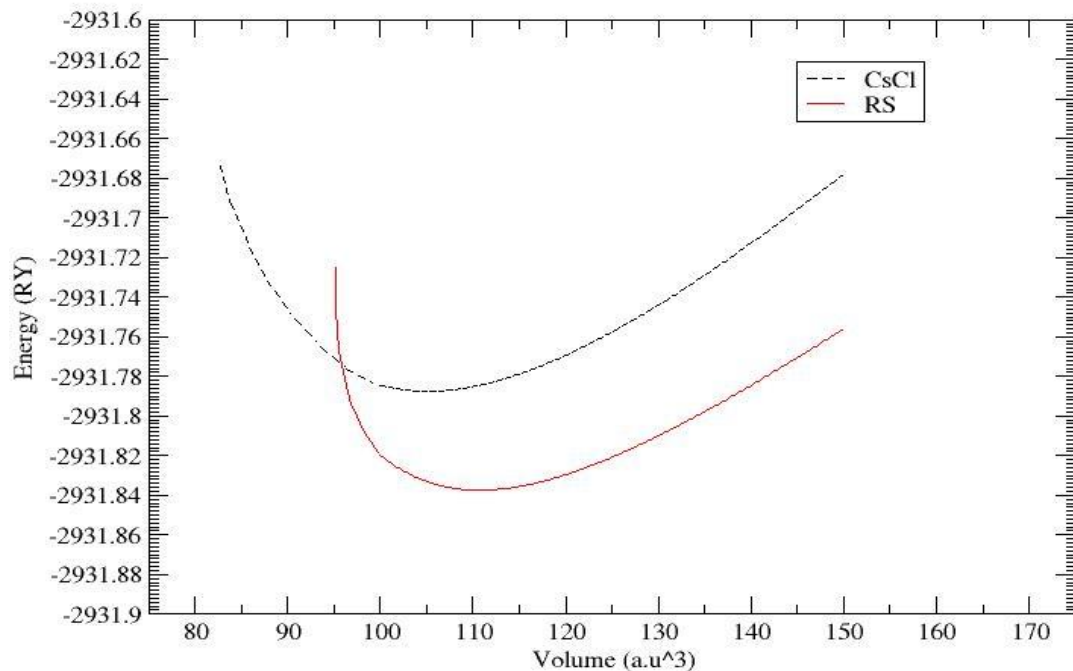


Figure 4.33 Equations of state for CoO in RS and CsCl structures by LDA method.

Figure 4.34 shows the EO'S for both RS & CsCl structures using W-Cohen method. The transition pressure was found to be 160.014 Gpa .

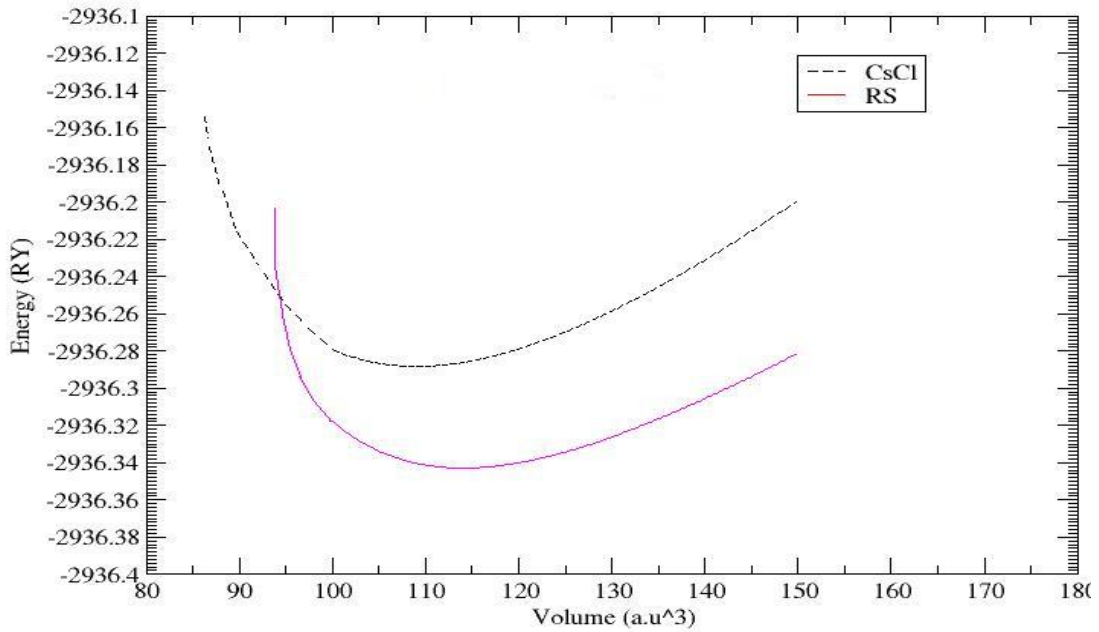


Figure 4.34 Equations of state for CoO in RS and CsCl structures by W-Cohen method.

Figure 4.35 shows the EO'S for both ZB & CsCl structures using GGA method. The transition pressure was found to be 35.35 Gpa .

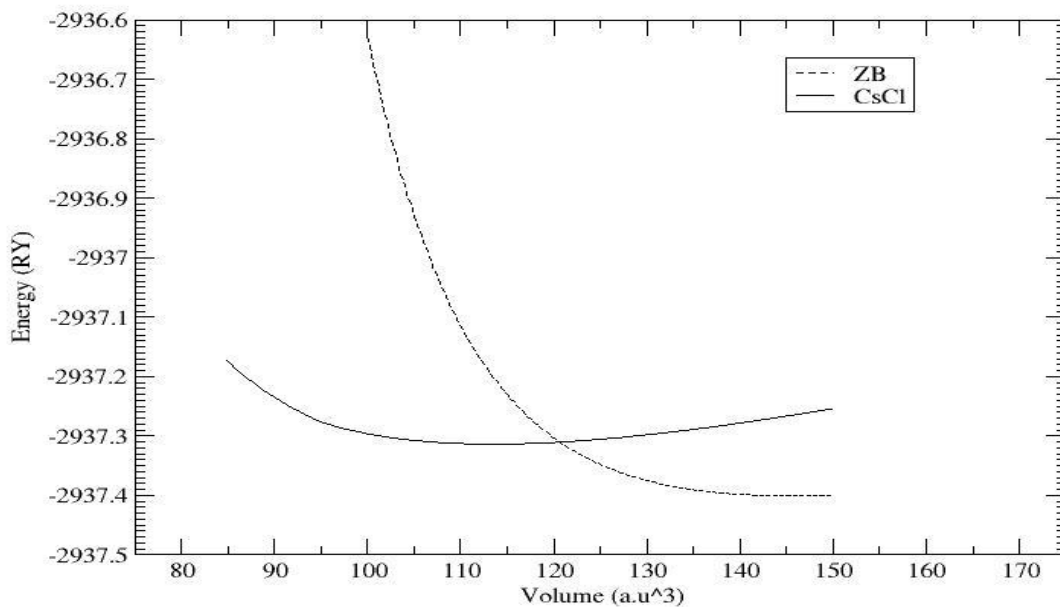


Figure 4.35 Equations of state for CoO in ZB and CsCl structures by GGA method.

Figure 4.36 shows the EO'S for both ZB & CsCl structures using LDA method. The transition pressure was found to be 37.66 Gpa .

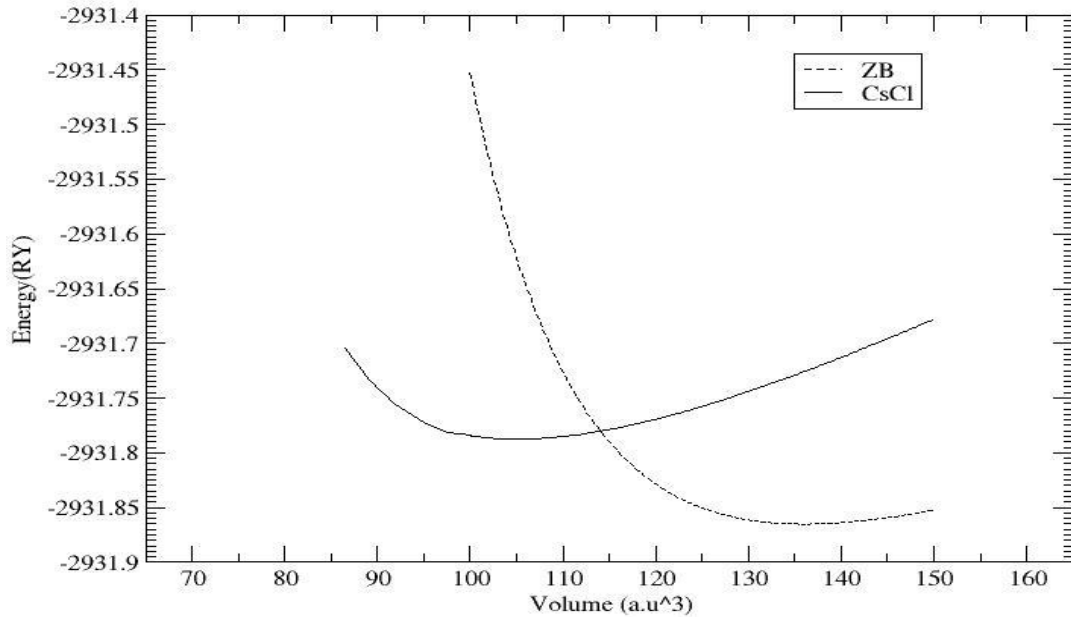


Figure 4.36 Equations of state for CoO in ZB and CsCl structures by LDA method.

Figure 4.37 shows the EO'S for both ZB & CsCl structures using W-Cohen method. The transition pressure was found to be 38.68 Gpa .

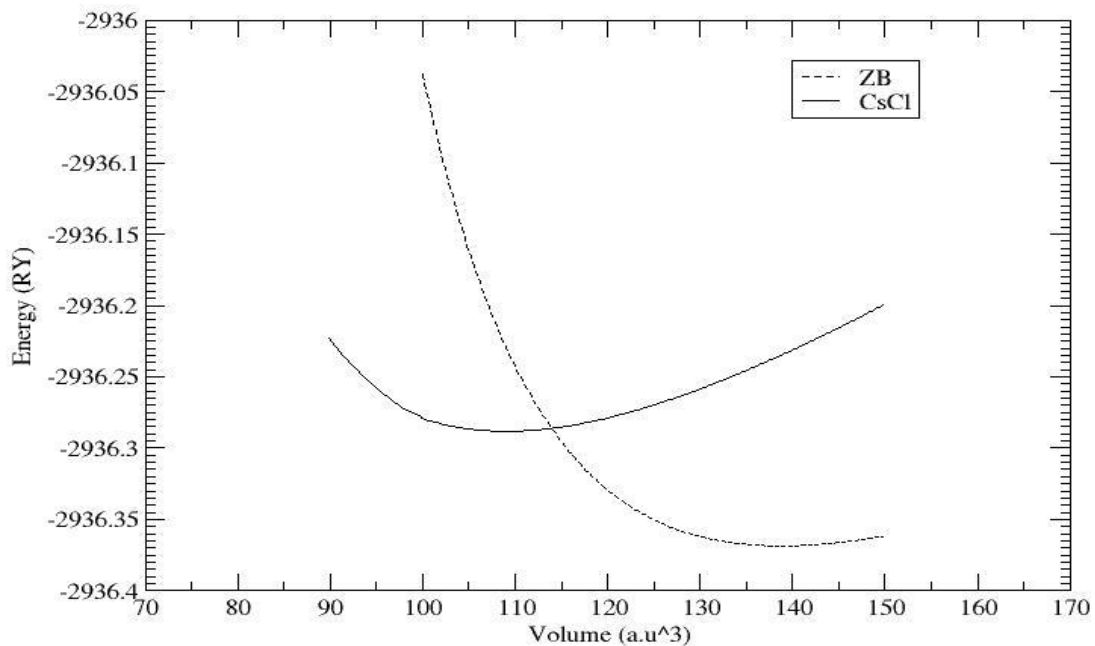


Figure 4.37 Equations of state for CoO in ZB and CsCl structures by W-Cohen method.

Figure 4.38 shows the EO'S for both RS & ZB structures using GGA method. The transition pressure was found to be 18.44 Gpa .

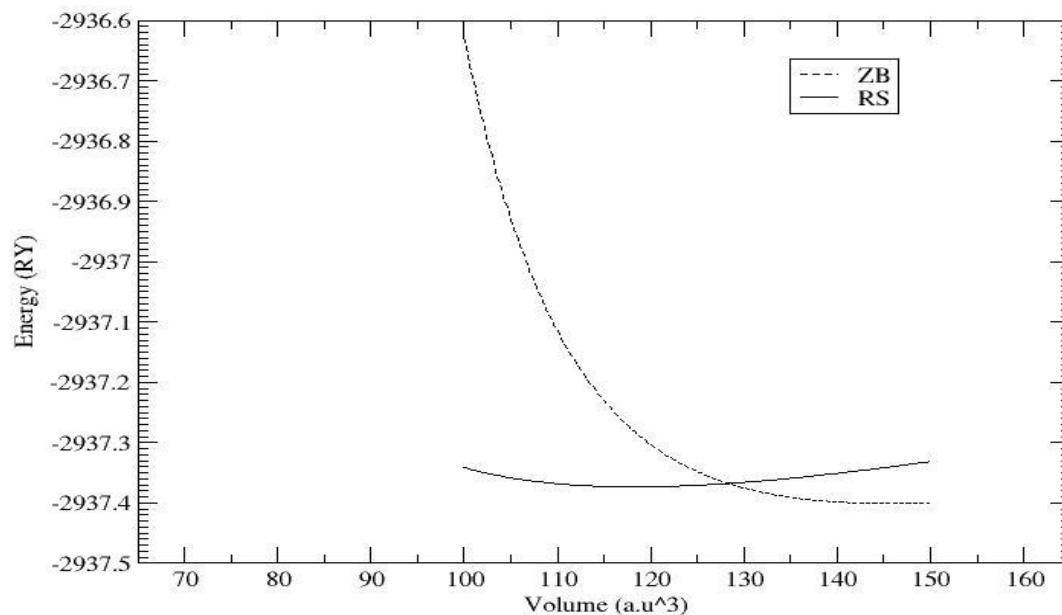


Figure 4.38 Equations of state for CoO in ZB and RS structures by GGA method.

Figure 4.39 shows the EO'S for both RS & ZB structures using LDA method. The transition pressure was found to be 16.54 Gpa .

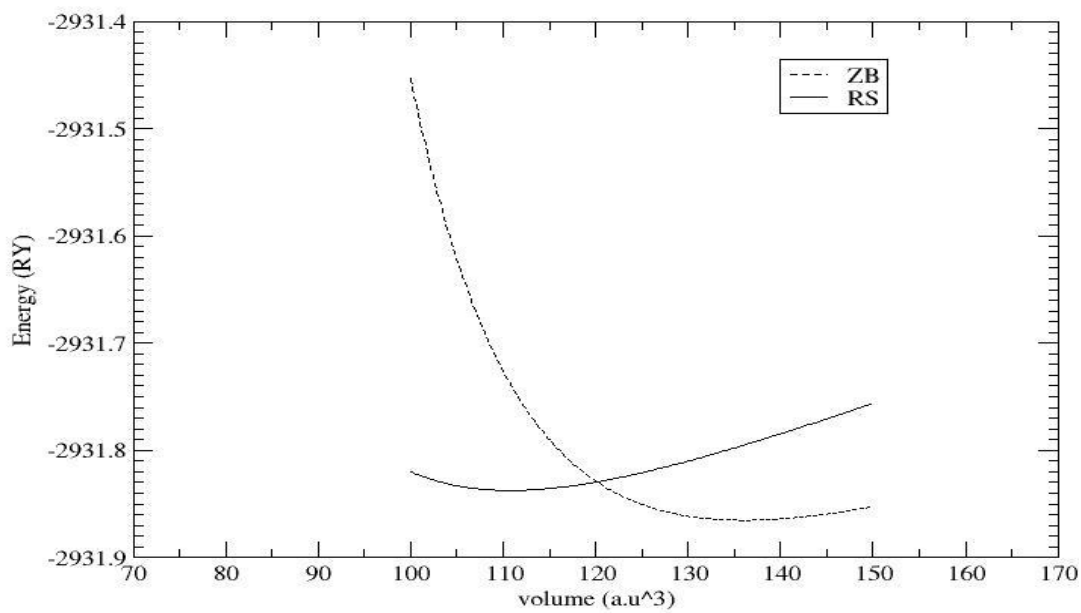


Figure 4.39 Equations of state for CoO in ZB and RS structures by LDA method.

Figure 4.40 shows the EO'S for both RS & ZB structures using W-Cohen method. The transition pressure was found to be 17.03 Gpa .

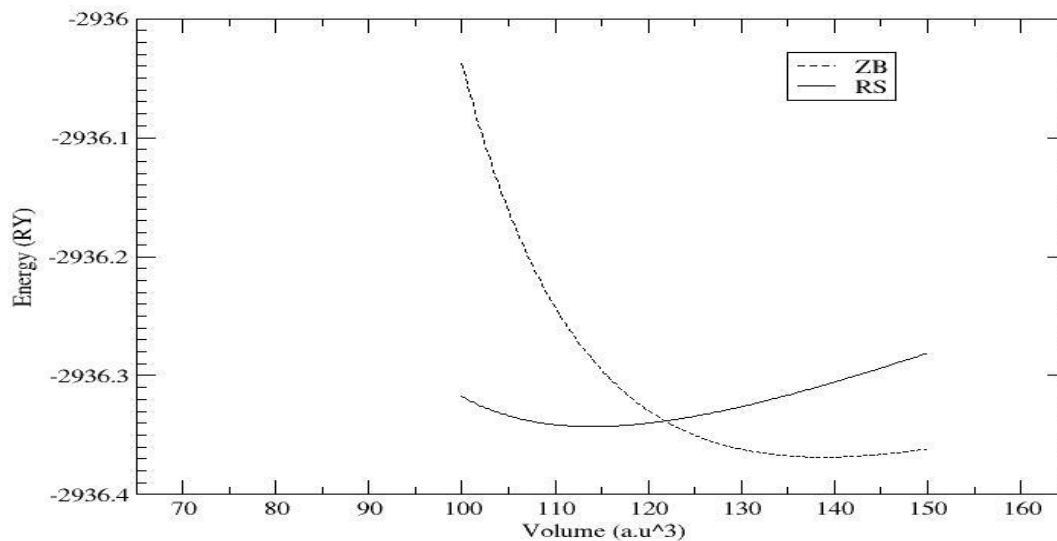


Figure 4.40 Equations of state for CoO in ZB and RS structures by W-Cohen method.

Figures 4.41, 4.42 and 4.43 show the four structures together on laid on one graph using LDA, GGA and W-Cohen methods . These graphs also show ZB structure is the ground state for CoO compound.

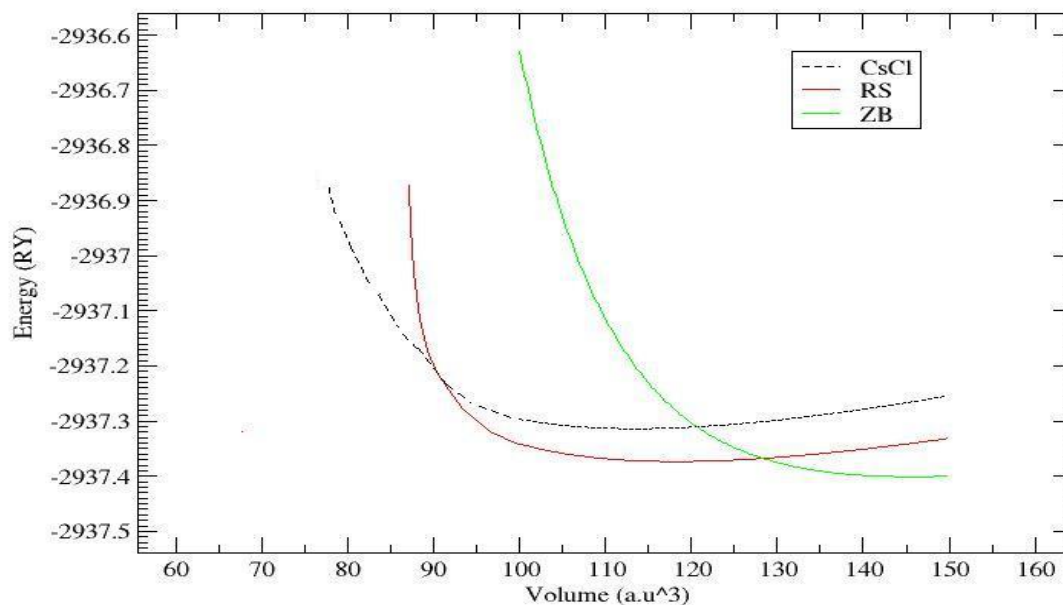


Figure 4.41 Equations of state for CoO in RS, CsCl and ZB structures by GGA method.

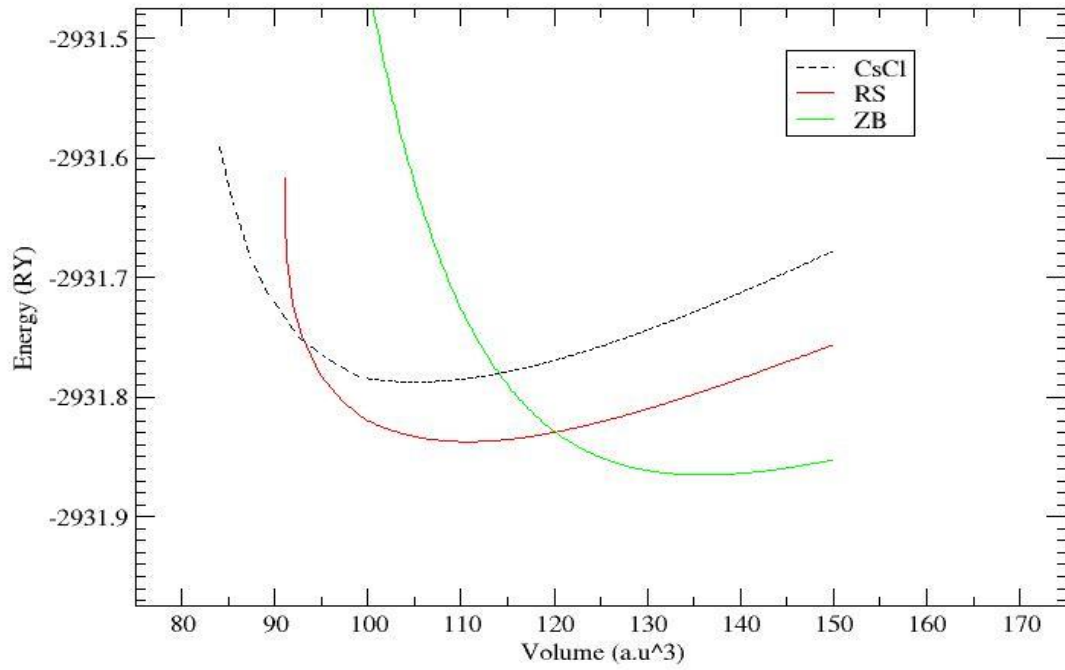


Figure 4.42 Equations of state for CoO in RS, CsCl and ZB structures by LDA method.

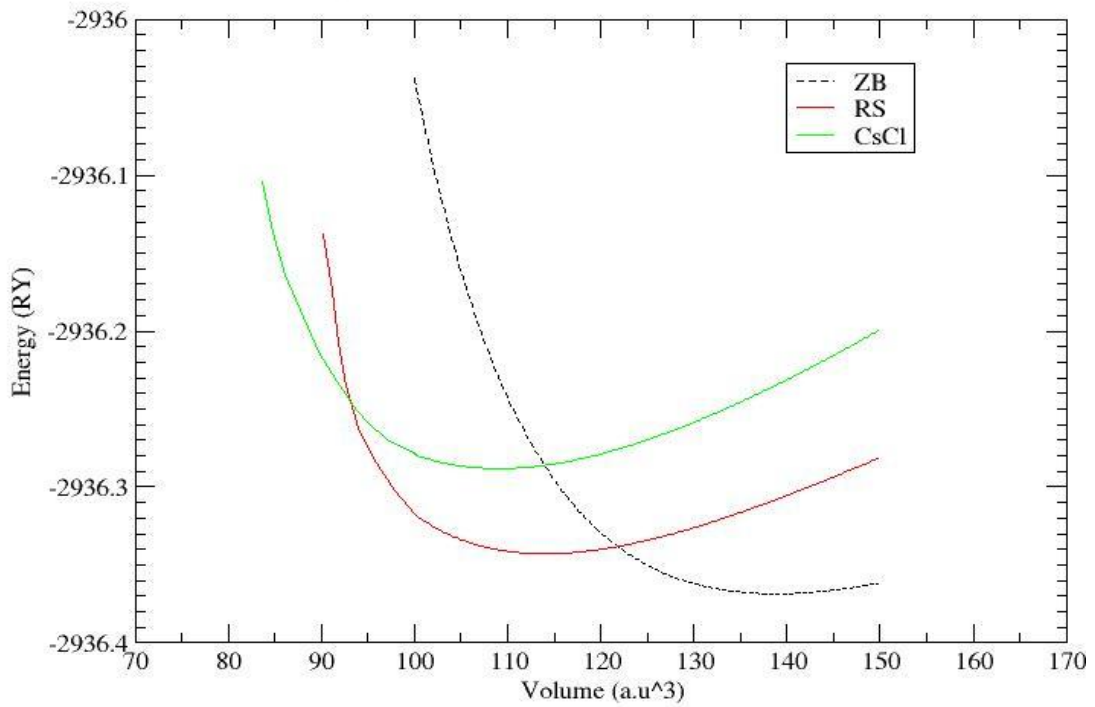


Figure 4.43 Equations of state for CoO in RS, CsCl and ZB structures by W-Cohen method.

Table 4.21 shows the value of the transition pressure between the phases of CoO compound.

Table 4.21 Transition pressure between the structures of CoO.

Transition	Studied parameter	present calculations		
		LDA	GGA	W-Cohen
RS-CsCl	Pt(Gpa)	104.206	126.78	160.014
ZB-CsCl	Pt(Gpa)	37.66	35.35	38.68
ZB-RS	Pt(Gpa)	16.54	18.44	17.03

Chapter Five

Conclusions

5.1 Introduction

In this thesis, the Full-Potential Augmented plane Wave (FP-LAPW) approach with LDA, GGA and W-Cohen methods is used to investigate the structural properties and stability of the WZ, ZB, CsCl and RS structures for CdO compound, and ZB, RS and CsCl phases for CoO compound, This method is also used to calculate the equation of state (EOS's) of (WZ), (ZB), (RS), and (CsCl) structures for both CdO and CoO compounds. From these (EOS's) the lattice parameter a , the bulk modulus B , the pressure derivative B' , the equilibrium volume of the crystal V_0 and the transition pressure P_t have been investigated. Also the energy band gaps were calculated using the same method for all structures mentioned above. The main results and conclusion of this study can be summarized as follows:

5.2 Structural parameters for CdO and CoO compounds

The calculations of structural parameters (a , B , B') and the minimum energy E using FP-LAPW approach with LDA, GGA and W-Cohen methods for CdO and CoO are found to be in good agreement with the available theoretical [12,48,51,52,54] and experimental [14,49,53,55] results. Tables 4.1, 4.2, 4.3 and 4.10 show these results of CdO compound for RS, CsCl, ZB and WZ phases respectively in GGA, LDA and W-Cohen approximations, while tables 4.17, 4.18 and 4.19 show these results of CoO compound, for RS, CsCl and ZB phases respectively.

5.3 The energy band gaps for CdO and CoO compounds

The studying of band structures and calculating the energy band gaps are very important for any material to determine whether this material is metal, semiconductor or insulator. The calculations of the energy band gaps are found to be in good agreement with the available theoretical results

5.3.1 The energy band gaps for CdO compound

The energy band gaps for CdO in RS structure with GGA, LDA, W-Cohen methods are found to be - 0.50047eV, - 0.44788 eV, - 0.52308 eV respectively, and for CdO in CsCl structure with GGA, LDA, W-Cohen are found to be -1.03891 eV , -1.28324 eV , -1.18536 eV respectively, but for CdO in ZB structure with GGA, LDA, W-Cohen are found to be almost zero eV for all phases. Finally for CdO in WZ structure with GGA, LDA, W-Cohen are found to be zero eV, but the other calculations are 0.66 eV[12] Table 4.11 shows these results.

5.3.2 Calculations of energy band gaps for CoO compound

The band gaps for CoO in RS structure with GGA, LDA, W-Cohen are found to be 0.01122 eV, 0.42596 eV, 0.14552 eV respectively, and for CoO in CsCl structure with GGA, LDA, W-Cohen are found to be 0.77975 eV , 1.0956 eV , 0.76518 eV respectively. Finally for CoO in ZB structure with GGA, LDA, W-Cohen are found to be - 0.54942 eV , - 0.17252 eV, -0.50409 eV respectively, but the other calculation is 2.5 eV [52]. Table 4.20 shows these results.

5.4 Transition pressure for CdO and CoO compounds

The lattice parameters should change from a structure to another under certain pressure which is called transition pressure . We found the value of this pressure from the slope of the graph energy versus volume for the two phases.

5.4.1 Transition pressure for CdO compound

The transition pressure for CdO compound occurs from RS to CsCl, WZ to CsCl, WZ to RS , ZB to CsCl, ZB to RS structure. The transition pressure from RS to CsCl was found 51.5 Gpa by GGA method, 72.57 Gpa by LDA method and 78.82 Gpa by W-Cohen method, but the transition pressure from WZ to CsCl was found 12.46 Gpa by GGA,13.74 Gpa by LDA,15.87 Gpa by W-Cohen, and the transition pressure from WZ to RS was found 3.7 Gpa by GGA,6.2 Gpa by LDA, the transition pressure also from ZB to CsCl was found 6.84 Gpa by GGA ,2.5 Gpa by LDA,5.67 Gpa by W-Cohen. Finally the transition pressure from ZB to RS was found 7.7 Gpa by GGA,1.85 Gpa by LDA, and no transition pressure from ZB to WZ structure. Table 4.12 Shows these results.

5.4.2 Transition pressure for CoO compound

The transition pressure for CoO compound occurs from RS to CsCl, ZB to RS and from ZB to CsCl structure. The transition pressure from RS to CsCl was found to 126.78 Gpa by GGA method, 104.206 Gpa by LDA method and 160.014 Gpa by W-Cohen method, but the transition pressure from ZB to RS was found 18.44 Gpa by GGA,16.54 Gpa by LDA,17.03 Gpa by W-Cohen. The transition pressure from ZB to CsCl was found to 35.35 Gpa by GGA method,

37.66 Gpa by LDA method, and 38.68 Gpa by W-Cohen method. Table 4.21 shows these results.

5.5 Ground state for CdO and CoO compounds

5.5.1 Ground state for CdO compound

The ground state for the CdO compound is RS structure. Tables 4.1, 4.2, 4.3 and 4.10 tables show the minimum energy for the structures of CdO compound. E is -11342.56863 Ry , -11342.56546 Ry , -11342.50854 Ry, -11342.6 Ry for RS , ZB , CsCl and W respectively by GGA approximations. The ground state for the CdO compound is RS structure.

5.5.2 Ground state for CoO compound

The ground state for CoO compound is ZB structure, tables 4.17, 4.18 and 4.19 show the minimum energy for the structures of CoO compound, E is -2937.373399 Ry , -2937.401025 Ry, -2937.313853 Ry for RS , ZB and CsCl respectively by GGA approximations. The ground state for the CoO compound is ZB structure.

5.6 Nature of CdO and CoO compounds

5.6.1 Nature of CdO compound

CdO compound behaves as a negative energy band gaps in RS and CsCl structures. Table 4.11 shows the energy band gaps for these structures. For RS the energy band gap is about - 0.500, - 0.448, - 0.523 eV by GGA, LDA and W-

Cohen approximations respectively. For CsCl the energy band gap is about -1.039, -1.283, -1.185 eV by GGA, LDA and W-Cohen approximations respectively. CdO compound behaves as semimetal in its structures ZB and WZ. For ZB the energy band gap is about 0.175, 0.127, 0.189 eV by GGA, LDA and W-Cohen approximations respectively. While for WZ the energy band gap is about 0.137, 0.139, 0.114 eV by GGA, LDA and W-Cohen approximations respectively, since this compound behaves as semimetal in RS, CsCl, ZB and WZ structures.

5.6.2 Nature of CoO compound

Table 4.20 shows the energy band gaps of CoO compound for its phases. For ZB the energy band gap is about -0.549, -0.173, -0.504 eV by GGA, LDA and W-Cohen approximations respectively. CoO compound behaves as semimetal in CsCl structure because the energy band gap is about 0.779, 1.096, 0.765 eV by GGA, LDA and W-Cohen approximations respectively. While for RS structure the energy band gap is about 0.011, 0.426, 0.146 eV by GGA, LDA and W-Cohen approximations respectively, which means that this compound behaves as semimetal in RS, CsCl, and ZB structures.

REFERENCES

- [1] Awolf, S., Awschlom, D.D., Buhrman R. A. 2001. **Science** **294**.
- [2] Bednorz, J.G., Mueller, K. A. 1986. **Phys. B. Condens Matter** **64**.
- [3] Fujimori, A., Mirani F. 1984. **Phys. Rev. B.** **30, 957**.
- [4], Sawatzky, G.A., Allen, J.W. 1987. **Phys. Rev. Lett.** **53, 2339**.
- [5] Hasse, M. A., Qui, L., Depuydt J. M., Luo H., Samarath N. 1991. **Phys. Lett.** **59, 1273**.
- [6] Gaines J., Drenten R., Haberen K. W., Marshall., Mensz P. M., Petruzzello J. 1993. **Phys. Lett.** **62, 2462**.
- [7] Fuchs M., Bockstede M., Pehlke E., Scheffler M. 1998. **Phys. Rev.** **B57, 2134**.
- [8] Nazzal A., Qteish A. 1996. **Phys. Rev. B** **53, 8262**.
- [9] Ristic, M., Popovic, S., Music, S. 2004. **Mater. Lett** **58, 2494**.
- [10] Gurumurugan, K., Mangalaraj, D. 1995. **Cryst. Growth** **147**.
- [11] Friberg, L., Piscator, M., Nordberg, G. F., Kjellstrom, T. 1974. **Cadmium in the Environment. 2nd ed.**
- [12] Schleife, A., Fuchs, F., Furthmuller, J., Bechstedt, F. 2006. **Phys. Rev.** **B 73, 245212**.
- [13] Jaffe, J. E., Snyder. J. A., Lin, Z., Hess, A. C. 2000. **Phys. Rev. B** **62, 1660**.
- [14] Liu, H., Mao, H., Somayazulu, M., Ding, Y., Meng, Y., Häusermann ,D . 2004. **phys. Rev. B** **70, 094114**.
- [15] Drickamer, H. G., Lynch, R. W., Clendenen, R. L. and Perez-Albuerne, E. A. 1966. **Solid State Phys.** **19, 135**.
- [16] Murnagham, F. D., Natl, P. 1994. **Acad. Sci. U.S.A.** **30, 244**.
- [17] Kadam, L. D., Patil, P. S., 2001. **Mater. Chem. Phys.** **68, P. 225**.

- [18] Fonseca, C. N., Depaoli, M. A., Gerenstein, A. 1994. **Sol. Energy Matter. Sol. cells 33, P.73.**
- [19] Seike, T., Nagai, J. 1991. **Sol. Energy Mater. 22, P. 107.**
- [20] Kim, H. K., Seong, T. Y., Lim, J. H., Cho, W. L., Yoon, Y. S. 2001. **Power Source. 102, P. 167.**
- [21] Seo. W. S., Shim, J. H., Oh, S. J. , Lee, E. K., Hur, N. H., Park, J. T. 2005. **Chem. Soc. 127, 6188.**
- [22] Atou, T., Kawsaki. M., Nakajima. S. 2004. **Apple. Phys. 43, L1281.**
- [23] Liu, J.F., He, Y., Chen, W., Zhang, G. Q., Zeng, Y. W., Jiang, J. Z. 2007. **Oho, Tsukuba. Japan. 305-0801. Phys. Chem. C 111, pp 2-5.**
- [24] Hedin, L., Lundqvist, S. 1969. **Solid State Physics, Vol. 23, p1.**
- [25] Blaha, P., Schwartz, K., Madsen, G. K., Kvasnicka. D., Luitz, J. 2001. **WIEN97. An Augmented Plane Wave + Local Orbital program For Calculating Crystal Properties, Karlheinz Schwartz, Techn. Universität Wien, Austria.**
- [26] Perdew, J. P., Levy, M.1983. **Phys. Rev. Lett. 51,1884.**
- [27] Coulson, C. 1960. **Rev. Mod . Phys. 32, 170.**
- [28] Fock, V., Physik. Z. 1930 . **Phys. Rev. 61, 126.**
- [29] Slater, J. C.1930. **Phys. Rev. 35, 210.**
- [30] Hohenberg, P., Kohn, W . 1964. Inhomogeneous electron gas, **Phys. Rev136B, 864-871.**
- [31] Kohn, W., Sham, L. S. 1965. **Self-consistent equations including exchange and correlation effects, Phys. Rev. 140, A1133-1138.**
- [32] Perdew, J. P., Burke, K., Ernzerhof, M. 1996. **Generalized Gradient Approximation made simple, Phys. Rev. Lett., 77, 3865-3868.**
- [33] Levy, M., Proc. 1979. **Nat. Acad. Sci. USA 76, 6062.**
- [34] Eschrig, H., Pikett. W. E. 2001. **Solid State Commun. 118, 123.**
- [35] Gaspar, R., Acta. 1954. **Phys. Hung. 3, 263.**

- [36] Gunnarsson, O., Lundqvist, B. I. 1976. **Phys. Rev. B** **13**, 4274.
- [37] Levy, M., Perdew, J. P. 1985. **Phys. Rev. A** **32**, 2010.
- [38] Hohenberg, P., Kohn, W. **Phys. Rev.** **136**, B 864.
- [39] Lieb, E.H. 1983. **Int. J. Quantum Chem.** **24**, 243.
- [40] Lieb, E. H. 1976. **Rev. Mod. Phys.** **48**, 553.
- [41] Perdew, J. P., Burke, S., Ernzerhof, M. 1997. **Phys. Rev. Lett.** **78**,
1386.
- [42] Anderson, O. K. 1975. **Phys. Rev.** **B12**, 3060.
- [43] Madsen, G. H., Blaha, P., Schwarz, K., Sjostedt, E., Nordstrom, L.
2001. **phys. Rev. B** **64**.
- [44] Singh, D. 1991. **Phys. Rev. B** **43**, 6388.
- [45] Blaha, P., Schwarz, K., Luitz, J. 1999. **WIEN97. A Full Potential
Linearized Augmented Plane Wave Package For Calculating
Crystal Properties** Karlheinz Schwartz, Techn. Universität Wien,
Austria.
- [46] http://www.sciencedaily.com/articles/c/crystal_structure.htm.
- [47] Needs, R. J. 2003. **Cambridge University, United kingdom. Phys.
Rev. Volume 75**.
- [48] Guerrero-Moreno, R. J., Takeuchi, N. 2002. **Phys. Rev.** **B66**, 205205.
- [49] Zhang, J. 1999. **Phys. Chem. Miner.** **26**, 644.
- [50] www.elsevier.com/locate/ssc.
- [51] Srivastava, V., Sanyal, S. P., Palagopalan, M. 2007. **Indian journal of
Pure & applied phys. Vol45, pp. 75-78**.
- [52] Tran, F., Blaha, P., Schwarz, K. 2006. **Phys. Rev.** **B74**, 155108.
- [53] Carey, M. J., Spada, F. E., Berkowitz, A. E., Cao, W., Thomas, G.,
Mater, J. 1991. **Res.** **6**, 2680.
- [54] Bredow, T., Gerson. A. R. 2000. **Phys. Rev. B** **61**. 5194.

- [55] Van Elp, J., Wieland, J. L., Eskes, H., Kuiper, P., Sawatzky, G. A., Degroot, F. M., Turner, T. S. 1991. **Phys. Rev. B** **44**. 6090.

جامعة النجاح الوطنية
كلية الدراسات العليا

حسابات FP-LAPW للخصائص الالكترونية و انتقالات الحالة التركيبية
لمركبات CdO و CoO

إعداد

كمال فلاح ناجي مصطفى

إشراف

د. محمد أبو جعفر

قدمت هذه الأطروحة استكمالاً لمتطلبات درجة الماجستير في الفيزياء بكلية الدراسات
العليا في جامعة النجاح الوطنية في نابلس، فلسطين.

2009

ب

حسابات FP-LAPW للخصائص الإلكترونية و انتقالات الحالة التركيبية لمركبات

CdO و CoO

إعداد

كمال فلاح ناجي مصطفى

إشراف

د. محمد أبو جعفر

الملخص

تتناول هذه الأطروحة دراسة بعض أكاسيد العناصر الانتقالية لما لها من أهمية كبيرة و بخاصة في المجالين الإلكتروني و الصناعي, حيث تناولنا دراسة مركبين من هذه الأكاسيد , هما أكسيد الكاديوم (CdO) و أكسيد الكوبالت (CoO), فقمنا بدراسة الخصائص البنيوية و البلورية لهذين المركبين, و من أهم هذه الخصائص , دراسة التركيب الإلكتروني, حساب مستويات الطاقة, إيجاد طاقة الفجوة التي من شأنها أن تحدد موصلية المركب (موصل, شبه موصل أو عازل). هناك طرق و أساليب كثيرة استخدمت في دراسة مثل هذه المركبات, لكننا اعتمدنا في دراستنا هذه أسلوب خاص يسمى (FP-LAPW) و الذي يعمل ضمن برنامج حاسوبي يسمى (WIEN2K) الذي يمكننا من استخدام أكثر من أسلوب تقريبي مثل (GGA), (LDA), و (W-Cohen). الجدير ذكره أن دراسة مثل هذه المركبات حاسوبيا أفضل بكثير من دراستها عمليا أو تجريبيا لعدة أسباب منها: المحافظة على الوقت و المال, و الحصول على نتائج دقيقة قليلة الخطأ. في دراستنا لمركبي (CdO) و (CoO) فقد تم حساب معادلة الحالة لكل التراكيب الممكنة لهما: (RS) Rocksalt, (CsCl) Cesium Chloride, Zinblende, (ZB) Wurtzite, (WZ). وتم تحديد أبعاد البلورة لكل تركيب من التراكيب السابقة, حساب الحجم والضغط الذي تتكون عنده كل بلوره ومن ثم تم حساب الضغط الانتقالي الذي تتحول عنده البلورة من تركيب إلى تركيب آخر, كما تم حساب مستويات الطاقة و إيجاد طاقة الفجوة لكل تركيب من المركبين.

من أهم نتائج هذه الدراسة :

1- تتراوح طاقة الفجوة لمركب CdO كما يلي: ما يقارب (0.13 eV) لتركيبية WZ و كذلك ما يقارب (0.17 eV) لتركيبية ZB . أما في تركيبية RS فإنها تقارب (-0.5 eV) و كذلك في تركيبية CsCl فإنها تقارب (-1.2 eV) مما يعني أن هذا المركب هو شبه معدن لجميع هذه التراكيب .

2- بينما تتراوح طاقة الفجوة لمركب CoO كما يلي: ما بين (0.11 - 0.77) إلكترون فولت لتركيبية CsCl . و كذلك فهي أيضا ما بين (-0.54 - -0.17) إلكترون فولت لتركيبية ZB . أما في تركيبية RS فإنها تقارب (0.01 eV) باستخدام الأسلوب التقريبي (GGA) , كذلك فإنها ما بين (0.15 - 0.42) إلكترون فولت باستخدام الأسلوب التقريبي LDA و W-Cohen مما يعني أن هذا المركب هو شبه معدن لجميع هذه التراكيب .

3- يمكن للتركيب أن ينتقل إلى تركيب آخر تحت ضغط معين.

4- تركيب (RS) هو التركيب الأساسي والطبيعي لمركب CdO عند درجات الحرارة العادية.

5- تركيب (ZB) هو التركيب الأساسي والطبيعي لمركب CoO عند درجات الحرارة العادية.

6- الحسابات التي حصلنا عليها تتطابق و بشكل كبير مع الحسابات النظرية والتجريبية السابقة.